IOPscience iopscience.iop.org

Home Search Collections Journals About Contact us My IOPscience

Functionals of Brownian motion, localization and metric graphs

This article has been downloaded from IOPscience. Please scroll down to see the full text article.

2005 J. Phys. A: Math. Gen. 38 R341

(http://iopscience.iop.org/0305-4470/38/37/R01)

View the table of contents for this issue, or go to the journal homepage for more

Download details:
IP Address: 171.66.16.94
The article was downloaded on 03/06/2010 at 03:57

Please note that terms and conditions apply.

INSTITUTE OF PHYSICS PUBLISHING JOURNAL OF PHYSICS A: MATHEMATICAL AND GENERAL

J. Phys. A: Math. Gen. **38** (2005) R341–R383 doi:10.1088/0305-4470/38/37/R01

TOPICAL REVIEW

Functionals of Brownian motion, localization and metric graphs

Alain Comtet[1,2], **Jean Desbois**[1] **and Christophe Texier**[1,3]

[1] Laboratoire de Physique Théorique et Modèles Statistiques, UMR 8626 du CNRS, Université Paris-Sud, Bât. 100, F-91405 Orsay Cedex, France
[2] Institut Henri Poincaré, 11 rue Pierre et Marie Curie, F-75005 Paris, France
[3] Laboratoire de Physique des Solides, UMR 8502 du CNRS, Université Paris-Sud, Bât. 510, F-91405 Orsay Cedex, France

Received 14 April 2005, in final form 28 July 2005
Published 31 August 2005
Online at stacks.iop.org/JPhysA/38/R341

Abstract

We review several results related to the problem of a quantum particle in a random environment. In an introductory part, we recall how several functionals of Brownian motion arise in the study of electronic transport in weakly disordered metals (weak localization). Two aspects of the physics of the one-dimensional strong localization are reviewed: some properties of the scattering by a random potential (time delay distribution) and a study of the spectrum of a random potential on a bounded domain (the extreme value statistics of the eigenvalues). Then we mention several results concerning the diffusion on graphs, and more generally the spectral properties of the Schrödinger operator on graphs. The interest of spectral determinants as generating functions characterizing the diffusion on graphs is illustrated. Finally, we consider a two-dimensional model of a charged particle coupled to the random magnetic field due to magnetic vortices. We recall the connection between spectral properties of this model and winding functionals of planar Brownian motion.

PACS numbers: 72.15.Rn, 73.20.Fz, 02.50.−r, 05.40.Jc, 05.45.Mt

(Some figures in this article are in colour only in the electronic version)

1. Introduction

1.1. Weak and strong localization

At low temperature, the electric conductivity σ of metals and weakly disordered semiconductors is determined by the scattering of electrons on impurities. It is given by the Drude formula

$$\sigma_0 = \frac{n_e e^2 \tau_e}{m}, \tag{1}$$

where e and m are the charge and mass of the electron respectively. n_e is the electronic density and τ_e the elastic scattering time[4]. This purely classical formula is only valid in a regime where quantum mechanical effects can be neglected. This is the case if the elastic mean free path of electrons $\ell_e = v_F \tau_e$ is large compared with the De Broglie wavelength $\lambda_F = 2\pi\hbar/mv_F$ corresponding to the Fermi energy (v_F is the Fermi velocity).

Strong localization. When these two length scales are of the same order $\ell_e \approx \lambda_F$ (strong disorder), the fact that the electrons are quantum objects must be taken into account and the wave-like character of these particles is of primary importance. It is indeed this wave character which is responsible for the localization phenomenon. The multiple scattering on impurities distributed randomly in space creates random phases between these different waves which can interfere destructively. These interference effects reduce the electronic conductivity. In the extreme case of very strong disorder, the waves no longer propagate and the system becomes insulating. This is the *strong localization* phenomenon which was conjectured by Anderson in 1958.

Weak localization. In the 1980s it was realized that even far from the strong localization regime the quantum transport is affected by the disorder. Diagrammatic techniques, used in the weak disorder limit $\lambda_F \ll \ell_e$, were initiated by the works of Al'tshuler, Aronov, Gor'kov, Khmel'nitzkiĭ, Larkin and Lee [12, 116] (see [13] for an introduction and [4] for a recent presentation). In this regime, called the *weak localization* regime, the Drude conductivity gets a small sample-dependent correction whose average, denoted by $\langle \Delta\sigma \rangle$, is called the 'weak localization correction'. $\langle \cdots \rangle$ denotes averaging with respect to the random potential. From the experimental side, this phenomenon is well established and has been the subject of many studies (see [34, 16] for review articles).

Phase coherence and dimensional reduction. The localization phenomenon comes from the interplay between the wave nature of electronic transport and the disorder. This manifestation of quantum interferences requires that the phase of the electronic wave is well defined; however, several mechanisms limit the phase coherence of electrons in metals, among which are the effect of the vibrations of the crystal (electron–phonon interaction) or the electron–electron interaction. We introduce a length scale L_φ, the phase coherence length, that characterizes the length over which phase breaking phenomenon becomes effective. The lack of phase coherence in real systems is the reason why the strong localization regime has not been observed in experiments on metals. In dimension $d = 3$ the strong localization regime is only expected to occur for sufficiently strong disorder[5]. However, strong localization can also be observed in the weak disorder limit ($\lambda_F \ll \ell_e$) by reducing the dimensionnality[6]. It has been shown in the framework of random matrix theory that the localization length of a weakly disordered quasi-1d wire behaves as $\lambda \sim N_c \ell_e$, where N_c is the number of conducting channels[7] [30, 79, 80, 166]. Therefore the strong localization regime is expected to occur

[4] The elastic scattering time τ_e is the time characterizing the relaxation of the direction of the momentum of the electron. The conductivity is proportional to τ_e for isotropic scattering by impurities. For anisotropic scattering the conductivity involves a different time $\tau_{\rm tr}$ called the 'transport' time [17] (see [4] for a discussion within the perturbative approach).

[5] Following the scaling ideas initiated by Thouless [156] and Wegner [219, 221] it was shown in [1] that the localization–delocalization transition exists only for dimension $d \geqslant 3$. In $d = 1$ and $d = 2$, the fully coherent system is always strongly localized, whatever the strength of the disorder.

[6] The effective dimension of the system is obtained by comparing the sample size with the phase coherence length L_φ. For example, a long wire of length L and of transverse dimension W is effectively in a 1d regime if $W \ll L_\varphi \ll L$.

[7] The localization length predicted by the random matrix theory (RMT) can be found in [30]: $\lambda_{\rm RMT} = [\beta(N_c - 1) + 2]\ell_e$, where $\beta = 1, 2, 4$ is the Dyson index describing orthogonal, unitary and symplectic ensembles,

when coherence is kept at least over a scale λ. At low temperature, in the absence of magnetic impurity, phase breaking mechanisms are dominated by electron–electron interaction, which leads to a divergence of the phase coherence length $L_\varphi(T) \propto (N_c/T)^{1/3}$ predicted in [9] and verified in several experiments such as [84, 213, 224] (see [180] for recent measurements down to 40 mK). Therefore the temperature below which strong localization might be observable is given by $L_\varphi(T_*) \sim \lambda$, which leads to $T_* \sim 1/\left(N_c^2 d\tau_e\right)$. The crossover temperature in metals is out of the experimental range, however it becomes reachable in wires etched at the interface of two semiconducting materials, when the number of conducting channels is highly reduced, and the manifestation of the strong localization has been observed in [109].

Strictly one-dimensional case. In a weakly disordered and coherent quasi-1d wire, the weak localization regime only occurs for length scales intermediate between the elastic mean free path and the localization length $\ell_e \ll L \ll \lambda$. In the strictly one-dimensional case, since $\lambda \simeq 4\ell_e$ for weak disorder[8], such a regime does not exist and the system is either ballistic ($\ell_e \gg L$) or strongly localized ($\ell_e \ll L$).

Anderson localization in one dimension has been studied by mathematicians and mathematical physicists from the view point of spectral analysis and in connection with limit theorems for products of random matrices [45]. A breakthrough was the proof of wave localization in one dimension by Gol'dshtein, Molchanov and Pastur [113]. Although some progress has been made, the multidimensional case is still out of reach and the subject of weak localization has almost not been touched in the mathematical literature. One of the main fields of interest in the last 20 years is the investigation of random Schrödinger operators in the presence of magnetic fields (see for example the [46, 77, 78, 100, 101, 220]; for recent results on Lifshitz tails with magnetic field see [101, 153]). From the physics side significant advances have been realized. Field theoretical methods based on supersymmetry provide a general framework for disordered systems and also allow establishing some links with quantum chaos [86].

While writing this review, we have tried to collect a large list of references which is however far from being exhaustive. Reference [157] provides a reference book on strong localization, mostly focused on spectrum and localization properties (see also [158] for a review on 1d discrete models and Lifshitz tails). A recent text about disorder and random matrix theory is [86]. Many excellent reviews have been written on weak localization, among them [34, 55] (for the role of disorder and electron–electron interaction, see the book [87] or [152]). A recent reference is [4].

1.2. Overview of the review

Section 2 shows that several functionals of the Brownian motion arise in the study of electronic transport in weakly disordered metals or semiconductors (weakly localized). The brief presentation of weak localization given in sections 2.1 and 2.2 follows the heuristic discussion of [13, 55], which is based on the picture proposed by Khmel'nitzkiĭ and Larkin. In spite of its heuristic character, it allows drawing suggestive connections with well-known functionals of the Brownian motion.

respectively. Note that one must be careful with the coefficient involved in this relation since the definitions of λ_{RMT} and ℓ_e differ slightly in RMT and in perturbation theory.

[8] The elastic mean free path $\ell_e = v_F\tau_e$ is given by the self-energy $1/(2\tau_e) = -\operatorname{Im}\Sigma^{\mathrm{R}}(E)$. For example, for a Gaussian disorder with local correlations, $\langle V(x)V(x')\rangle = w\delta(x-x')$, we obtain $1/\tau_e \simeq 2\pi\rho_0 w$ for a weak disorder, where ρ_0 is the free density of states. In one dimension $\rho_0 = 1/(\pi v_F)$, therefore $\ell_e \simeq v_F^2/(2w)$, which coincides with the *high energy* (weak disorder) expansion of the localization length $\lambda \simeq 2v_F^2/w$ [15, 157].

Sections 3 and 4 deal with problems of strong localization in one dimension. A powerful approach to handle such problems is the phase formalism[9] (presented in [15, 157] for instance). This formalism leads to a broad variety of stochastic processes. Section 3 discusses scattering properties of a random potential, and section 4 studies spectral properties of a Schrödinger operator defined on a finite interval.

In section 5, we review some results obtained for networks of wires (graphs), which can be viewed as systems of intermediate dimension between one and two. We will put the emphasis on spectral determinants, which appear to be an efficient tool to construct several generating functions characterizing the diffusion on graphs (or its discrete version, the random walk).

Finally, in section 6, we show that the physics of a two-dimensional quantum particle submitted to the magnetic field of an assembly of randomly distributed magnetic vortices involves fine properties of planar Brownian motion.

2. Functionals of Brownian motion in the context of weak localization

2.1. Feynman paths, Brownian motion and weak localization

In the path integral formulation of quantum mechanics, each trajectory is weighted with a phase factor $\mathrm{e}^{\mathrm{i}S/\hbar}$ where S is the classical action evaluated along this trajectory. The superposition principle states that the amplitude of propagation of a particle between two different points is given by the sum of amplitudes over all paths connecting these two points. This formulation of quantum mechanics is most useful when there is a small parameter with respect to which one can make a quasiclassical expansion. One encounters a similar situation in the derivation of geometrical optics starting from wave optics. In this case the small parameter is the ratio of the wave length to the typical distances which are involved in the problem and the classical paths are light rays. In the context of weak localization the small parameter is λ_F/ℓ_e and the quasiclassical approximation amounts to sum over a certain subset of Brownian paths. The fact that Brownian paths come into the problem is not so surprising if one goes back to our previous physical picture of electrons performing random walks due to scattering by impurities. In the continuum limit, describing the physics at length scales much larger than ℓ_e, this random walk may be described as a Brownian motion. It can be shown that $\langle \Delta\sigma \rangle$ is related to the time integrated probability for an electron to come back to its initial position (see [55] for a heuristic derivation or [4] for a recent derivation in space representation):

$$\langle \Delta\sigma \rangle = -\frac{2e^2 D}{\pi\hbar} \int_{\tau_e}^{\infty} \mathrm{d}t\, \mathcal{P}(\vec{r}, t|\vec{r}, 0)\, \mathrm{e}^{-t/\tau_\varphi}, \tag{2}$$

where D is the diffusion constant and the factor 2 accounts for spin degeneracy. $\mathcal{P}(\vec{r}, t|\vec{r}', 0)$ is Green's function of the diffusion equation

$$\left(\frac{\partial}{\partial t} - D\Delta\right) \mathcal{P}(\vec{r}, t|\vec{r}', 0) = \delta(\vec{r} - \vec{r}')\delta(t). \tag{3}$$

In equation (2) the exponential damping at large time describes the lack of phase coherence due to inelastic processes. The phase coherence time τ_φ can be related to the phase coherence length by $L_\varphi^2 = D\tau_\varphi$. We have also introduced a cut-off at short time in equation (2) that takes into account the fact that the diffusion approximation is only valid for times larger than τ_e.

[9] The phase formalism is a continuous version of the Dyson–Schmidt method [83, 188]. A nice presentation can be found in [158].

2.2. Planar Brownian motion: stochastic area, winding and magnetoconductance

Weak localization corrections are directly related to the behaviour of the probability of return to the origin and thus to recurrence properties of the diffusion process. It therefore follows that dimension $d = 2$ plays a very special role. Consider for instance a thin film whose thickness a is much less than L_φ. The sample is effectively two dimensional and the correction to the conductivity is given by

$$\langle \Delta\sigma \rangle = -\frac{e^2}{\pi^2 \hbar} \ln(L_\varphi/\ell_e). \tag{4}$$

On probabilistic grounds the logarithmic scaling is of course not unexpected here, it is the same logarithm which occurs in asymptotic laws of planar Brownian motion [151, 181]. The neighbourhood recurrence of planar Brownian motion favours quantum interference effects and leads to a reduction of the electrical conductivity. A more striking effect is predicted if one applies a constant and homogeneous magnetic field $\mathcal{B}$ over the sample. In this case the classical action contains a coupling to the magnetic field $S = e\mathcal{B}A$ where A is a functional of the path given by the line integral

$$A = \frac{1}{2} \int (x\, \mathrm{d}y - y\, \mathrm{d}x). \tag{5}$$

Properly interpreted, this line integral is nothing but the stochastic area of planar Brownian motion, whose distribution was first computed by P Lévy before the discovery of the Feynman path integral. The weak localization correction reads

$$\langle \Delta\sigma(\mathcal{B}) \rangle - \langle \Delta\sigma(0) \rangle = \frac{e^2}{2\pi^2 \hbar} \int_0^\infty \frac{\mathrm{d}t}{t}\, \mathrm{e}^{-t/\tau_\varphi} (1 - \mathrm{E}[\mathrm{e}^{2\mathrm{i}e\mathcal{B}A/\hbar}]). \tag{6}$$

The coupling to the magnetic field now appears with an additional factor 2 coming from the fact that the weak localization describes quantum interferences of reversed paths. The expectation $\mathrm{E}[\cdots]$ is taken over Brownian loops for a time t. The magnetoconductivity is given by [12, 34, 55]

$$\langle \Delta\sigma(\mathcal{B}) \rangle - \langle \Delta\sigma(0) \rangle = \frac{e^2}{2\pi^2 \hbar} \left[\psi\left(\frac{1}{2} + \frac{\phi_0}{8\pi \mathcal{B} L_\varphi^2} \right) - \ln\left(\frac{\phi_0}{8\pi \mathcal{B} L_\varphi^2} \right) \right] \simeq \frac{4}{3} \frac{e^2}{\hbar} \left(\frac{\mathcal{B} L_\varphi^2}{\phi_0} \right)^2, \tag{7}$$

where $\psi(z)$ is the digamma function and $\phi_0 = h/e$ is the quantum flux. The rhs corresponds to the weak field limit $\mathcal{B} \ll \phi_0 / L_\varphi^2$. This increase of the conductivity with magnetic field is opposite to the behaviour expected classically. This phenomenon is called 'positive (or anomalous) magnetoconductance'. Experimentally this effect is of primary importance: the magnetic field dependence allows one to distinguish the weak localization correction from other contributions and permits us to extract the phase coherent length L_φ. This expression fits the experimental results remarkably well[10] [34].

Strictly speaking equation (7) only holds for an infinite sample. In the case of bounded domains the variance depends on the geometry of the system and can be computed explicitly for rectangles and strips [76]. The case of inhomogeneous magnetic fields can be treated along the same line. Consider for instance a magnetic vortex carrying a flux ϕ and threading the sample at point 0. In this case the functional which is involved is not the stochastic area but the index of the Brownian loop with respect to 0 (winding number). The probability distribution of the index has been computed independently by Edwards [85] in the context of polymer physics and Yor [227] in relation to the Hartman–Watson distribution. For a planar

[10] Note that in materials with strong spin–orbit scattering, such as gold, the effect is reversed and a negative magnetoconductance is observed at small magnetic fields [34, 127].

Brownian motion started at r and conditioned to hit its starting point at time 1, the distribution of the index when n goes to infinity is

$$\text{Proba}[\text{Ind} = n] \simeq \frac{1}{2\pi^2 n^2} K_0(r^2)\, \mathrm{e}^{-r^2}, \tag{8}$$

where $K_0(x)$ is the modified Bessel function of second kind (MacDonald function). The fact that the even moments of this law are infinite is reflected in the non-analytic behaviour of the conductivity

$$\langle \Delta\sigma(\phi)\rangle - \langle \Delta\sigma(0)\rangle \propto |\phi|. \tag{9}$$

It is interesting to compare with equation (7) where the quadratic behaviour is given by the second moment of the stochastic area [169]. The behaviour given by equation (9) has been observed experimentally [31, 107] and a theoretical interpretation is provided in [182].

2.3. Dephasing due to electron–electron interaction and functionals of Brownian bridges

2.3.1. Dephasing in a wire: relation with the area below a Brownian bridge. Another interesting example of a non-trivial connection between a physical quantity and a functional of Brownian motion occurs in the study of electron–electron interaction and weak localization correction in a quasi-1d metallic wire. In [9], Al'tshuler, Aronov and Khmel'nitzkiĭ (AAK) proposed to model the effect of the interaction between an electron and its surrounding environment by the interaction with a fluctuating classical field. The starting point is a path integral representation of the probability $\mathcal{P}(\vec{r}, t|\vec{r}', 0)$ in which is included the effect of the fluctuating field that brings a random phase. After averaging over Gaussian fluctuations of the field, given by the fluctuation–dissipation theorem, AAK obtained

$$\langle \Delta\sigma\rangle = -2\frac{e^2 D}{\pi S_{\mathrm{w}}} \int_0^\infty \mathrm{d}t\, \mathrm{e}^{-\gamma t} \int_{x(0)=x}^{x(t)=x} \mathcal{D}x(\tau) \times \exp\left(-\frac{1}{4D}\int_0^t \mathrm{d}\tau \dot{x}(\tau)^2 - \frac{e^2 T}{\sigma_0 S_{\mathrm{w}}} \int_0^t \mathrm{d}\tau |x(\tau) - x(t-\tau)|\right), \tag{10}$$

where T is the temperature (the Planck and Boltzmann constants are set equal to unity $\hbar = k_B = 1$), and S_{w} is the area of the section of the quasi-1d wire. In contrast with equation (2) where the loss of phase coherence was described phenomenologically by an exponential damping[11] with the parameter τ_φ, here the electron–electron interaction affects the weak localization correction through the introduction in the action of the functional of the Brownian bridge[12]

$$\widetilde{\mathcal{A}}_t = \int_0^t \mathrm{d}\tau |x(\tau) - x(t-\tau)|. \tag{11}$$

The additional damping $\exp -\gamma t$ in equation (10) describes the loss of phase coherence due to other phase breaking mechanisms. By using a trick which makes the path integral local in time, AAK have computed explicitly the path integral and obtained:

$$\langle \Delta\sigma\rangle = \frac{e^2}{\pi S_{\mathrm{w}}} L_N \frac{\mathrm{Ai}(\gamma\tau_N)}{\mathrm{Ai}'(\gamma\tau_N)}, \tag{12}$$

[11] Note that the introduction of an exponential damping describes rigorously several effects: the loss of phase coherence due to spin–orbit scattering or spin-flip [127], the penetration of a weak perpendicular magnetic field in a quasi-1d wire [8]. In this latter case the effect of the magnetic field is taken into account through $\gamma = \frac{1}{3}(e\mathcal{B}W)^2$ where W is the width of the wire of rectangular section.

[12] A Brownian bridge, $(x(\tau), 0 \leqslant \tau \leqslant 1 | x(0) = x(1))$, is a Brownian path conditioned to return to its starting point.

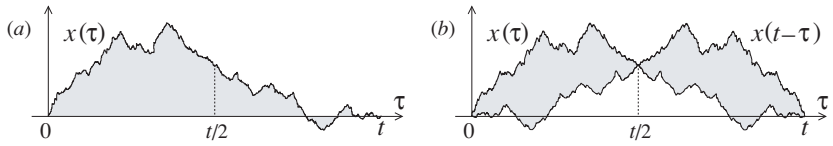

Figure 1. Left: the functional $\mathcal{A}_t$ gives the absolute area below a Brownian bridge $x(\tau)$. Right: The functional $\widetilde{\mathcal{A}}_t$ measures the area between the Brownian bridge $x(\tau)$ and its time reversed counterpart $x(t-\tau)$. The two functionals are equal in law (equation (14)).

where $\mathrm{Ai}(z)$ is the Airy function. The Nyquist time, $\tau_N = \left(\frac{\sigma_0 S_w}{e^2 T\sqrt{D}}\right)^{2/3}$, gives the time scale over which electron–electron interaction is effective and therefore plays the role of a phase coherence time. We have also introduced the corresponding length $L_N = \sqrt{D\tau_N}$. Note that the T dependence of $\tau_N \propto T^{-2/3}$ directly reflects the scaling of the area with time: $\widetilde{\mathcal{A}}_t \overset{(\mathrm{law})}{=} t^{3/2}\widetilde{\mathcal{A}}_1$. We stress that the AAK theory makes a quantitative prediction for the dependence of the phase coherence length L_N as a function of the temperature, which has been verified experimentally for a wide range of parameters: on metallic (gold) wires [84, 180] (the behaviour of $L_N \propto (S_w/T)^{1/3}$ was observed before in aluminium and silver wires [224]), and on wires etched at the interface of two semiconductors [213].

It is interesting to point out that the result of AAK can be interpreted as the Laplace transform of the distribution of the functional (11), $\mathrm{E}[\exp -p\widetilde{\mathcal{A}}_t]$. This functional represents the area between a Brownian bridge and its time reversed counterpart (cf figure 1(*b*)), where $\mathrm{E}[\cdots]$ describes averaging over Brownian bridges. The conjugate parameter p is played in (10) by the temperature: $p = \frac{e^2 T}{\sigma_0 S_w}$. Result (12) has also been derived in the probability literature. Let us consider the functional

$$\mathcal{A}_t = \int_0^t \mathrm{d}\tau |x(\tau)|, \tag{13}$$

giving the absolute area below the Brownian bridge starting from the origin, $x(0) = x(t) = 0$ (cf figure 1(*a*)). The double Laplace transform of the distribution of $\mathcal{A}_t$ has been computed first by Cifarelli and Regazzini [58] in the context of economy and independently by Shepp [195], and led to $\int_0^\infty \frac{\mathrm{d}t}{\sqrt{t}}\,\mathrm{e}^{-\gamma t}\mathrm{E}[\mathrm{e}^{-\sqrt{2}\mathcal{A}_t}] = -\sqrt{\pi}\,\frac{\mathrm{Ai}(\gamma)}{\mathrm{Ai}'(\gamma)}$, which is equivalent[13] to the result (12). The connection between the two results is clear from the equality in law [14]:

$$\mathcal{A}_t \overset{(\mathrm{law})}{=} \widetilde{\mathcal{A}}_t \tag{14}$$

which follows from[15]

$$x(\tau) - x(t-\tau) \overset{(\mathrm{law})}{=} x(2\tau) \qquad \text{for} \quad \tau \in [0, t/2]. \tag{15}$$

Relation (14) allows us to understand more deeply the trick used by AAK to make the path integral (10) local in time. The distribution of the area $\mathcal{A}_t$ has been also studied by Rice in [183]. Interestingly, the inverse Laplace transform of equation (12) obtained by Rice has been rederived recently independently in [168] in order to analyse the loss of phase coherence due to electron–electron interaction in a time representation.

[13] Note that the $1/\sqrt{t}$ in the integral computed by Shepp corrects the fact that the averaging over Brownian curves in (10) is not normalized to unity, whereas $\mathrm{E}[\cdots]$ is.

[14] For a given process $x(\tau)$ the two functionals $\mathcal{A}_t$ and $\widetilde{\mathcal{A}}_t$ are obviously different, however they are distributed according to the same probability distribution. They are said 'equal in law'.

[15] Relation (15) is easily proved by using that a Brownian bridge $(x(\tau), 0 \leqslant \tau \leqslant 1 | x(0) = x(1) = 0)$ can be written in terms of a free Brownian motion $(B(\tau), \tau \geqslant 0 | B(0) = 0)$ as $x(\tau) = B(\tau) - \tau B(1)$.

The study of statistical properties of the absolute area below a Brownian motion was first addressed by Kac [135] for a free Brownian motion, long before the case of the Brownian bridge studied by Cifarelli and Regazzini and by Shepp. Later on, it has been extended to other functionals of excursions and meanders[16] [133, 179], which arise in a number of seemingly unrelated problems such as computer science, graph theory [95] and statistical physics [160, 161].

2.3.2. Dephasing in a ring. Very recently, the question of dephasing due to electron–electron interaction in a weakly disordered metal has been raised again in [159]. In particular it has been shown that the effect of the geometry of the ring and the effect of electron–electron interaction combine in a non-trivial way leading to a behaviour of the harmonics of the magnetoconductance that differs from that predicted by equation (2) in [10]. For the ring, the functional describing the effect of electron–electron interaction on weak localization is now given by

$$\mathcal{R}_t = \int_0^t \mathrm{d}\tau |x(\tau)| \left(1 - \frac{|x(\tau)|}{L}\right) \tag{16}$$

instead of the area defined by equation (13). $x(\tau)$ is a Brownian path[17] on a ring of perimeter L such that $x(0) = x(t) = 0$. The question has been re-examined in more detail in [211], where the double Laplace transform of the distribution $\int_0^\infty \mathrm{d}t\, \mathrm{e}^{-\gamma t} \frac{1}{\sqrt{t}} \mathrm{e}^{-\frac{(nL)^2}{2t}}\ \mathrm{E}_n[\mathrm{e}^{-\mathcal{R}_t}]$ has been derived. $\mathrm{E}_n[\cdots]$ denotes averaging over Brownian bridges defined on a circle, with winding number n. Note that the Laplace transform of the distribution $\mathrm{E}_n[\mathrm{e}^{-\mathcal{R}_t}]$ has been also studied in [211].

3. Exponential functionals of Brownian motion and Wigner time delay

3.1. Historical perspective

Exponential functionals of the form,

$$A_t^{(\mu)} = \int_0^t \mathrm{d}s \exp -2(B(s) + \mu s) \tag{17}$$

where $(B(s), s \geqslant 0, B(0) = 0)$ is an ordinary Brownian motion have been the object of many studies in mathematics [228], mathematical finance and physics [64]. In the physics of classical disordered systems, the starting point was the analysis of the series (Kesten variable)

$$Z = z_1 + z_1 z_2 + z_1 z_2 z_3 + \cdots \tag{18}$$

where the z_i are independent and identical random variables. Several papers have been devoted to the study of this random variable in the physics [68, 71] and mathematics [138, 217] literature. It was realized that Z is the discretized version of $A_\infty^{(\mu)}$ defined in equation (17), which may be interpreted as a trapping time in the context of classical diffusion in a random medium. The tail of the probability distribution $P(Z)$ controls the anomalous diffusive behaviour of a particle moving in a one-dimensional random force field [42]. The functional $A_t^{(\mu)}$ also arises in the study of the transport properties of disordered samples of finite length

[16] An excursion is a part of a Brownian path between two consecutive zeros and a meander is the part of the path after the last zero.

[17] As for the case of the wire, the functional involved in the study of dephasing in the ring [211] involves the difference $x(\tau) - x(t - \tau)$ instead of the bridge $x(\tau)$. We have used the equality in law (15) which implies the following property: given a Brownian bridge $(x(\tau), 0 \leqslant \tau \leqslant t | x(0) = x(t) = 0)$, for any even function $f(x)$ we have $\int_0^t \mathrm{d}\tau f(x(\tau) - x(t - \tau)) \overset{(\mathrm{law})}{=} \int_0^t \mathrm{d}\tau f(x(\tau))$.

[170, 173]. In the context of one-dimensional localization the fact that the norm of the wavefunction is distributed[18] as $A_\infty^{(1)}$ is mentioned in the book of Lifshitz *et al* [157].

3.2. Wigner time delay

As discussed in the introduction, the localization of quantum states in one dimension is well understood. However since real systems are not infinite, asking about the nature of the states which are not in the bulk is a perfectly legitimate question. It was pointed out by Azbel in [21] that, when a disordered region is connected to a region free of disorder, the localized states acquire a finite lifetime which shows up in transport through sharp resonances, referred to as 'Azbel resonances'. This picture was used in [132] where it was argued that these resonances could be probed in scattering experiments and lead to an energy-dependent random time delay of the incident electronic wave. Motivated by this result and by developments in random matrix theory we consider the scattering problem for the one-dimensional Schrödinger equation (in units $\hbar = 2m = 1$)

$$-\frac{\mathrm{d}^2}{\mathrm{d}x^2}\psi(x) + V(x)\psi(x) = E\psi(x) \tag{19}$$

defined on the half line $x \geqslant 0$ with the Dirichlet boundary conditions $\psi(0) = 0$. The potential $V(x)$ has its support on the interval $[0, L]$. Outside this interval, the scattering state of energy $E = k^2$ is given by

$$\psi_E(x) = \frac{1}{\sqrt{hv_E}}(\mathrm{e}^{-\mathrm{i}k(x-L)} + \mathrm{e}^{\mathrm{i}k(x-L)+\mathrm{i}\delta}), \tag{20}$$

where $h = 2\pi$ is the Planck constant (in unit $\hbar = 1$) and $v_E = \mathrm{d}E/\mathrm{d}k = 2k$ the group velocity. Equation (20) represents the superposition of an incoming plane wave incident from the right and a reflected plane wave characterized by its phase shift $\delta(E)$. The Wigner time delay, defined by the relation $\tau = \mathrm{d}\delta/\mathrm{d}E$, can be understood as the time spent by the wave packet of energy E in the disordered region (this interpretation is only valid at high energy; see [50, 69, 125, 149] for review articles on time delay and traversal times). This representation of the time delay has been used in many papers both in the mathematics and physics literature. Starting from this representation one can derive a system of stochastic differential equations which can be studied in certain limiting cases. However, to understand the universality of the statistical properties of the Wigner time in the high-energy limit, we follow a different approach below.

3.2.1. Universality of time delay distribution at high energy. Using the expression of the scattering state (20) and the definition $\tau = \mathrm{d}\delta/\mathrm{d}E$, we can obtain the so-called Smith formula [98, 196] relating the time delay to the wavefunction in the bulk:

$$\tau(E) = 2\pi \int_0^L \mathrm{d}x|\psi_E(x)|^2 - \frac{1}{2E}\sin\delta(E). \tag{21}$$

Following [15] one can parametrize the wavefunction in the bulk in terms of its phase and modulus. For this purpose we rewrite the Schrödinger equation as a set of two coupled first order differential equations, $\mathrm{d}\psi_E/\mathrm{d}x = \psi'_E$ and $\mathrm{d}\psi'_E/\mathrm{d}x = (V(x) - E)\psi_E$, and perform the change of variables: $\psi_E(x) = \mathrm{e}^{\xi(x)}\sin\theta(x)$ and $\psi'_E(x) = k\,\mathrm{e}^{\xi(x)}\cos\theta(x)$. One obtains a new set of first-order differential equations $\mathrm{d}\theta/\mathrm{d}x = k - \frac{1}{k}V(x)\sin^2\theta$ and $\mathrm{d}\xi/\mathrm{d}x = \frac{1}{2k}V(x)\sin 2\theta$.

[18] When $\mu > 0$, $A_t^{(\mu)}$ possesses a limit distribution for $t \to \infty$. Moreover, we have the equality in law (see footnote 14): $A_\infty^{(\mu)} \overset{\text{(law)}}{=} 1/\gamma^{(\mu)}$, where $\gamma^{(\mu)}$ is distributed according to a Γ-law: $P(\gamma) = \frac{1}{\Gamma(\mu)}\gamma^{\mu-1}\,\mathrm{e}^{-\gamma}$.

Up till now everything is exact. If we now consider the high energy limit[19] we can neglect the second term on the rhs of equation (21) and integrate out the phase which is a fast variable; we obtain

$$\tau = \frac{1}{k}\int_0^L \mathrm{d}x\, \mathrm{e}^{2(\xi(x)-\xi(0))}. \tag{22}$$

This representation of the time delay holds for any realization of the disordered potential. Moreover, one can prove under rather mild conditions on the correlations of the random potential that $\xi(x)$ is a Brownian motion with drift $\xi(x) = x/\lambda + \sqrt{1/\lambda}B(x)$ where $B(x)$ is an ordinary Brownian motion and λ the localization length. Using the scaling properties of Brownian motion gives the following identity in law

$$\tau \overset{(\mathrm{law})}{=} \frac{\lambda}{k}\int_0^{L/\lambda} \mathrm{d}x\, \mathrm{e}^{-2(B(x)+x)} = \frac{\lambda}{k}A^{(1)}_{L/\lambda}, \tag{23}$$

where $A^{(1)}_L$ has been defined in equation (17). This representation of the time delay as an exponential functional of Brownian motion, first established in [93] by a different method, allows us to obtain a number of interesting results [65, 207]:

(i) Existence of a limit distribution for fixed[20] τ and $L \to \infty$

$$P(\tau) = \frac{\lambda}{2k\tau^2}\,\mathrm{e}^{-\frac{\lambda}{2k\tau}}. \tag{24}$$

This result is reminiscent of the random matrix theory prediction in spite of the fact that this theory does not apply to systems that are strictly one dimensional[21].

(ii) Linear divergence of the first moment, $\langle\tau\rangle = L/k$, and exponential divergence of the higher moments $\langle\tau^n\rangle \propto \mathrm{e}^{2n(n-1)L/\lambda}$. This divergence reflects a log–normal tail of the distribution for a finite length L.

3.2.2. Time delay and density of states. Relation (21) also provides another interpretation to these results. In the situation under consideration, the scattering state is directly related to the local density of states (LDoS) by $\rho(x; E) = \langle x|\delta(E - H)|x\rangle = |\psi_E(x)|^2$. Therefore the time delay can be interpreted as the DoS of the disordered region[22]. This establishes a relation between the results given above and the work of Al'tshuler and Prigodin [14] where the distribution of the LDoS was studied for a white noise potential using the method of Berezinskiĭ[23].

3.2.3. Time delay for Dirac Hamiltonian at the threshold energy. The representation (23) of the time delay as an exponential functional of the Brownian motion only holds in the weak

[19] To define precisely the high-energy limit, let us introduce the integral of the correlation function of the disorder $w = \int \mathrm{d}x\langle V(x)V(0)\rangle$. The high-energy limit corresponds to $k \gg w^{1/3}$.

[20] From the remark of footnote 18, we note that $1/\tau$ is distributed according to an exponential law.

[21] The random matrix theory describes the regime of weak localization or systems whose classical dynamics is chaotic. The distribution of time delay in this framework has the same functional form $P(\tau) \propto \frac{1}{\tau^{2+\mu}}\,\mathrm{e}^{-\tau_0/\tau}$ [47, 102, 114, 174] with two differences: (i) the exponent $2 + \mu > 2$, (ii) the time scale τ_0.

[22] The relation between time delay and DoS is sometimes referred as Krein–Friedel relation [97, 144]. This relation has originally been introduced in [37] in the context of statistical physics (see also [67] and section 77 of [148]). Note that it has recently been discussed in the context of graphs in [205, 206, 208].

[23] The method of Berezinskiĭ blocks has been introduced to study specifically the case of white noise disordered potential in one dimension [32]. This powerful approach has been widely used and has allowed us to derive numbers of important results like in [112, 115] for example.

disorder (i.e. high energy) limit. A similar representation can be derived for the random mass Dirac model at the middle of the spectrum. The Dirac Hamiltonian is

$$H_{\mathrm{D}} = \sigma_2 \mathrm{i}\frac{\mathrm{d}}{\mathrm{d}x} + \sigma_1 \phi(x), \tag{25}$$

where σ_i are the Pauli matrices. $\phi(x)$ can be interpreted as a mass[24]. The Dirac equation $H_{\mathrm{D}}\psi = k\psi$ possesses a particle–hole symmetry reflected in the symmetry of the spectrum with respect to $k = 0$ (the dispersion relation of the Dirac equation is linear in the absence of the mass term and energy is equal to momentum). The middle of the spectrum is an interesting point where the divergence in the localization length signals the existence of a delocalized state (see footnote 31). These properties should therefore show up in the probability distribution of the Wigner time delay. Since the dispersion relation of the Dirac equation is linear, the time delay is now defined as $\tau = \mathrm{d}\delta/\mathrm{d}k$. The following representation has been derived in [198]:

$$\tau = 2\int_0^L \mathrm{d}x \exp\left(2\int_0^x \phi(y)\,\mathrm{d}y\right). \tag{26}$$

In contrast with equations (22) and (23), which have been obtained after averaging over the fast phase variable, the representation (26) is exact (for $k = 0$). If $\phi(x)$ is a white noise, then

$$\tau = \frac{2}{g}A_{gL}^{(0)}. \tag{27}$$

In this case since the drift vanishes, it is known [170, 228] that there is no limiting distribution when $L \to \infty$. The physical meaning of the log–normal tail

$$P(\tau) \sim \frac{1}{2\tau\sqrt{2\pi gL}}\,\mathrm{e}^{-\frac{1}{8gL}\ln^2(g\tau)} \tag{28}$$

in the limit $\tau \to \infty$ is discussed in detail in [198].

4. Extreme value spectral statistics

The density of states (DoS) and the localization length of a one-dimensional Hamiltonian with a random potential can be studied by the phase formalism [15, 157] (see also [158] for discrete models). In the previous section we pointed out that the physics of the strong localization in one dimension can also be probed from a different angle by considering the scattering of a plane wave by the random potential. This has led to the study of the Wigner time delay. In this section we show that the phase formalism also allows describing finer properties of the spectrum such as the probability distribution of the nth eigenvalue. This is an instance of an *extreme value statistics*: given a ranked sequence of $\mathcal{N}$ random variables $x_1 \leqslant x_2 \leqslant \cdots \leqslant x_{\mathcal{N}}$, the problem is to find the distribution of the nth of these variables in a given interval. In the particular case of uncorrelated random variables, the extreme value distributions have been studied by E Gumbel [119–121]. This problem becomes much more complicated when the random variables are correlated, a case which has recently attracted a lot of attention. Such extreme value problems have appeared recently in a variety of problems ranging from disordered systems [44, 54, 70] to certain computer science problems such as growing search trees [162]. In the case of the spectrum of a random Hamiltonian, the eigenvalues are in general

[24] The Hamiltonian (25) with $\phi(x)$ a white noise was introduced by Ovchinnikov and Erikmann [176] as a model of a one-dimensional semiconductor with a narrow fluctuating gap. It is interesting to point out that the Dirac equation $H_{\mathrm{D}}\psi = k\psi$ also has an interpretation in the context of superconductivity, as linearized Bogoliubov–de Gennes equations for a real random superconducting gap $\phi(x)$. Finally it is worth mentioning that more general 1d Dirac Hamiltonians with several kinds of disorder (mass term, potential term and magnetic field) have been studied in [38, 39].

correlated variables, apart from the case of strongly localized eigenstates [167]. Below we show that, in the one-dimensional case, this problem is related to studying the first exit time distribution of a one-dimensional diffusion process.

4.1. Distribution of the nth eigenvalue: relation with a first exit time distribution

We consider a Schrödinger equation $H\varphi(x) = E\varphi(x)$ on a finite interval $[0, L]$. The spectral (Sturm–Liouville) problem is further defined by imposing suitable boundary conditions. We choose the Dirichlet boundary conditions $\varphi(0) = \varphi(L) = 0$. The spectrum of H is denoted by $\mathrm{Spec}(H) = \{E_0 < E_1 < E_2 < \cdots\}$. Our purpose is to compute the probability

$$W_n(E) = \langle \delta(E - E_n) \rangle \tag{29}$$

for the eigenvalue E_n to be at energy E (the bracket $\langle \cdots \rangle$ means averaging over the random potential). Note that the sum of these distributions $\frac{1}{L}\sum_n W_n(E) = \rho(E)$ is the average DoS per unit length. We now show how the calculation of $W_n(E)$ can be cast into a first exit time problem.

4.1.1. Random Schrödinger Hamiltonian. We consider the Hamiltonian

$$H = -\frac{\mathrm{d}^2}{\mathrm{d}x^2} + V(x), \tag{30}$$

where $V(x)$ is a Gaussian white noise random potential: $\langle V(x) \rangle = 0$ and $\langle V(x)V(x') \rangle = w\delta(x - x')$.

We replace the Sturm–Liouville problem by a Cauchy problem: let $\psi(x; E)$ be the solution of the Schrödinger equation $H\psi(x; E) = E\psi(x; E)$ with the boundary conditions $\psi(0; E) = 0$ and $\frac{\mathrm{d}}{\mathrm{d}x}\psi(0; E) = 1$. The boundary condition $\psi(L; E) = 0$ is fulfilled whenever the energy E coincides with an eigenvalue E_n of the Hamiltonian. In this case, the wavefunction $\varphi_n(x) = \psi(x; E_n) \big/ \big[\int_0^L \mathrm{d}x' \psi(x'; E_n)^2 \big]^{1/2}$ has n nodes in the interval $]0, L[$, and two nodes at the boundaries.

Let us denote by ℓ_m ($m \geqslant 1$), the length between two consecutive nodes. We consider the Ricatti variable

$$z(x; E) = \frac{\mathrm{d}}{\mathrm{d}x} \ln |\psi(x; E)|, \tag{31}$$

which obeys the following equation:

$$\frac{\mathrm{d}}{\mathrm{d}x} z = -E - z^2 + V(x), \tag{32}$$

with initial condition $z(0; E) = +\infty$. This equation may be viewed as a Langevin equation for a particle located at z submitted to a force $-\partial U(z)/\partial z$ deriving from the unbounded potential

$$U(z) = Ez + \frac{z^3}{3} \tag{33}$$

and to a random white noise $V(x)$.

Each node of the wavefunction corresponds to $|z(x)| = \infty$. At 'time' $x = 0$ the 'particle' starts from $z(0) = +\infty$ and eventually ends at $z(\ell_1 - 0^+) = -\infty$ after a 'time' ℓ_1. Just after the first node it then starts again from $z(\ell_1 + 0^+) = +\infty$, due to the continuity of the wavefunction. It follows from this picture that the distance ℓ_m between two consecutive nodes may be viewed as the 'time' needed by the particle to go through the interval $]-\infty, +\infty[$ (the 'particle' is emitted from $z = +\infty$ at initial 'time' and absorbed when it reaches $z = -\infty$).

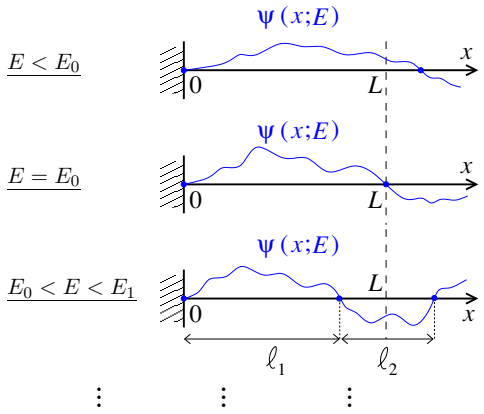

Figure 2. The probability for the nth level E_n of the spectrum to be at E is also the probability for the $(n+1)$th node of $\psi(x;E)$ to be at L.

The distances ℓ_m are random variables, interpreted as times needed by the process z to go from $+\infty$ to $-\infty$. These random variables are statistically independent because each time the variable z reaches $-\infty$, it loses the memory of its earlier history since it is brought back to the same initial condition and $V(x)$ is δ-correlated. This remark is a crucial point for the derivation of $W_n(E)$. Interest in these random 'times' ℓ_m lies in their relation with the distribution of the eigenvalues. Indeed the probability that the energy E_n of the nth excited state is at E is also the probability that the sum of the $n+1$ distances between the nodes is equal to the length of the system: $L = \sum_{m=1}^{n+1} \ell_m$ (this is illustrated in figure 2). Since the ℓ_m are independent and identically distributed random variables Prob$\left[L = \sum_{m=1}^{n+1} \ell_m\right]$ is readily obtained from the distribution $P(\ell)$ of one of these variables.

We introduce the intermediate variable $\mathcal{L}(z)$ giving the time needed by the process starting at z to reach $-\infty$: therefore we have $\ell = \mathcal{L}(+\infty)$. The Laplace transform of the distribution $h(\alpha, z) = \langle \mathrm{e}^{-\alpha\mathcal{L}} \mid z(0) = z;\ z(\mathcal{L}) = -\infty \rangle$ obeys [105]

$$G_z h(\alpha, z) = \alpha h(\alpha, z), \tag{34}$$

where the backward Fokker–Planck generator is

$$G_z = -U'(z)\partial_z + \frac{w}{2}\partial_z^2. \tag{35}$$

The boundary conditions are $\partial_z h(\alpha, z)|_{z=+\infty} = 0$ and $h(\alpha, -\infty) = 1$. By Laplace inversion we can derive $P(\ell)$ since $h(\alpha, +\infty) = \int_0^\infty \mathrm{d}\ell\, P(\ell)\, \mathrm{e}^{-\alpha\ell}$.

The solution of this problem is given in [204]. Here we only consider the limit $E \to -\infty$, which corresponds to the bottom of the spectrum. In this regime the dynamics of the Ricatti variable z can be read off from the shape of the potential (see figure 3).

The particle falls rapidly into the well from which it can only escape by a fluctuation of the random force. Therefore the time needed to go from $+\infty$ to $-\infty$ is dominated by the time spent in the well, which is distributed according to the Arrhenius formula. It follows that the average 'time', which is related to the inverse of the integrated density of states (IDoS) per unit length $N(E) = \int_0^E \mathrm{d}E' \rho(E')$, behaves as $\langle \ell \rangle = N(E)^{-1} \simeq \frac{\pi}{\sqrt{-E}} \exp \frac{8}{3w}(-E)^{3/2}$. This simple picture, first provided by Jona–Lasinio [134], allows recovering of the exponential tail

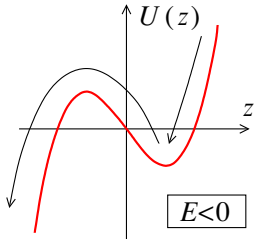

Figure 3. The potential (33) related to the deterministic force to which the Ricatti variable is submitted in equation (32).

obtained by several methods in [15, 99, 124, 130, 157][25]. The distribution of the length ℓ is a Poisson law (see [105] or the appendix of [204]):

$$P(\ell) = N(E) \exp -\ell N(E). \tag{36}$$

Using this result we can show that [204]

$$W_n(E) = L\rho(E) \frac{(LN(E))^n}{n!} \mathrm{e}^{-LN(E)}. \tag{37}$$

This result has a clear meaning: $L\rho(E)$ gives the probability of finding any level at E and the factor $\frac{x^n}{n!}\,\mathrm{e}^{-x}$ 'compels' the number of states below E, $x = LN(E)$, to be close to n. We may go further and write

$$W_n(E) = \frac{1}{\delta E_n} \omega_n \left(\frac{E - E_n^{\mathrm{typ}}}{\delta E_n} \right), \tag{38}$$

where the typical value of the energy is $E_n^{\mathrm{typ}}(L) = -\left(\frac{3w}{8} \ln \tilde{L}\right)^{2/3}$, while the scale of the fluctuations reads $\delta E_n = \frac{w^{2/3}}{2\sqrt{n+1}} (3 \ln \tilde{L})^{-1/3}$, where $\tilde{L} = \frac{L w^{1/3}}{2\pi(n+1)}$. The function

$$\omega_n(X) = \frac{(n+1)^{n+\frac{1}{2}}}{n!} \exp\left(\sqrt{n+1}\, X - (n+1)\mathrm{e}^{X/\sqrt{n+1}}\right) \tag{39}$$

has the form of a Gumbel law for *uncorrelated* random variables. The fact that the eigenvalues are uncorrelated is a consequence of the strong localization of the eigenfunctions [167].

The work summarized in the above paragraph, which appeared in [204], generalizes the result of McKean [165] for the ground state.

A similar result was obtained by Grenkova *et al* [117] for the model of δ-impurities with random positions, in the limit of low impurity density which has no counterpart in the model we considered here[26]. However both models describe the same physics of strongly localized eigenstates.

4.1.2. Supersymmetric random Hamiltonian. Random Schrödinger operators have been investigated through a wide range of models. Depending on the physical context, there are indeed many ways to model the disorder. In the previous section we have assumed that the potential $V(x)$ is a white noise. We have also mentioned that if the potential is a superposition of δ-potentials randomly distributed along the line, although the spectra of the two models are

[25] It is interesting to quote [145] where it was shown that this non-perturbative exponential tail can be obtained by a simple counting method of 'skeleton' diagrams assuming that they all have the same value (this approach was also applied to the 3d case).

[26] See footnote 27.

quite different[27], the extreme spectral statistics are the same. The localization properties and the statistics of the time delay at high energy are also similar for both models [203, 207]. These two models belong to the same class of random Hamiltonians with a random scalar potential with short-range correlations. They are both continuous versions of discrete tight binding models with on-site random potential. This is the case of so-called *diagonal disorder*, since the random potential appears on the diagonal matrix elements of the tight binding Hamiltonian on the basis of localized orbitals[28].

Other interesting models can be constructed by introducing disorder in the hoppings, instead. We refer to such models as *off-diagonal disorder*. The Dirac Hamiltonian (25) introduced above provides a continuum limit of such a model[29]. Dirac Hamiltonians appear naturally in several contexts of condensed matter physics. The existence of symmetries in the Dirac Hamiltonian[30] (particle–hole, chiral, ...) can lead to interesting features in the presence of disorder, which has attracted some attention (see for example [7, 39, 40, 48, 49, 88, 172]; reference [88] gives a brief overview). The square of the Dirac Hamiltonian, $H_{\mathrm{D}}^2 = -\mathrm{d}_x^2 + \phi(x)^2 + \sigma_3\phi'(x)$, is related to the pair of supersymmetric Schrödinger isospectral Hamiltonians $H_\pm = -\mathrm{d}_x^2 + \phi(x)^2 \pm \phi'(x)$. When $\langle\phi(x)\rangle = 0$ we may forget the sign and simply consider:

$$H_S = -\frac{\mathrm{d}^2}{\mathrm{d}x^2} + \phi(x)^2 + \phi'(x). \tag{40}$$

Such Hamiltonians appear in a variety of problems ranging from the 1d classical diffusion in a random force [42, 128], electronic structure of polyacetylene [200], spin Peierls chains [91, 92, 199] and also in a continuum limit of the random field XY model [122] (see [66] for a short review on supersymmetric disordered quantum mechanics). Spectral and localization properties have been studied in detail when $\phi(x)$ is a white noise [41, 42, 157, 176] and also when $\phi(x)$ has a finite correlation length as in a random telegraph process [61] (this last case has found some application in the context of spin Peierls chains).

In the high-energy limit, the localization properties and the statistics of the time delay do not show any difference with respect to the case of diagonal disorder. However the low-energy properties are quite different. This is easily understood by noting that, due to its relation to the Dirac Hamiltonian, the supersymmetric Hamiltonian can be factorized as $H_S = Q^\dagger Q$ where $Q = -\mathrm{d}_x + \phi(x)$ and $Q^\dagger = \mathrm{d}_x + \phi(x)$. In particular, such a structure enforces a positive spectrum: $\mathrm{Spec}(H_S) \subset \mathbb{R}^+$. When $\phi(x)$ is white noise of zero mean, $\langle\phi(x)\rangle = 0$ and $\langle\phi(x)\phi(x')\rangle = g\delta(x - x')$, the case considered below, the DoS presents a logarithmic Dyson

[27] The model of δ-impurities with random positions was introduced and studied by Schmidt [188] but often referred as the Frisch and Lloyd model [99]. Compared to the model for white noise potential, which is characterized by one parameter, the Frisch & Lloyd model is characterized by two parameters: the strength of the δ-potential, and their density. In the limit of high density of impurities this model is equivalent to the white noise potential model. The limit of low density presents different spectral singularities (Lifshitz singularity and, for negative weight of δ-potentials, an additional Halperin singularity in the negative part of the spectrum).

[28] Note that the continuum limit of tight binding Hamiltonian with diagonal disorder can lead to different continuous models. Let us consider the discrete model $H_{i,j} = -\delta_{i,j+1} - \delta_{i,j-1} + \delta_{i,j}V_i$. For $V_i = 0$ the spectrum is $E_k = -2\cos(k)$, with $k \in]-\pi, \pi]$. (A) If the continuous limit is taken by considering the band edge ($k \sim 0$), one is led to the continuous model (30). (B) If the band centre is considered instead ($k \sim \pi/2$), the spectrum can be linearized and one is led to a Dirac Hamiltonian, as in [137, 176]. This point has been recently rediscussed in [189].

[29] The continuum limit of a tight binding Hamiltonian with random hoppings has been discussed in [200] (see also the review in [169]). As pointed in footnote 28, random Dirac Hamiltonians can also appear as continuum limit of the band centre of a discrete models with diagonal disorder.

[30] A complete classification of symmetries of disordered Hamiltonians extending the famous Wigner–Dyson ensembles of random matrix theory has been provided in [7, 216, 229] (see also the recent review article [126]).

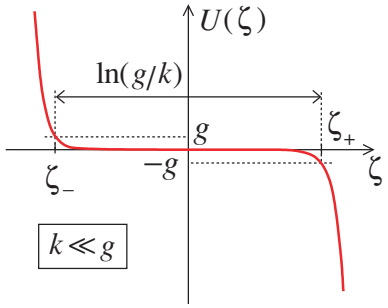

Figure 4. The potential related to the deterministic force in equation (43) felt by the variable ζ.

singularity: the integrated density of states (IDoS) reads $N(E) \sim 1/\ln^2 E$ [41, 42, 176], while the localization length diverges logarithmically[31] $\lambda(E) \sim \ln(1/E)$.

It is interesting to investigate the extreme value statistics of the spectrum in the low-energy regime, where we expect properties quite different from that obtained for the diagonal disorder. The derivation follows closely that in the previous case, however the relevant random processes and the approximations are different. The first step is to decouple the Schrödinger equation $H_S\varphi(x) = k^2\varphi(x)$ into two first-order differential equations (i.e. go back to the Dirac equation):

$$Q^\dagger \chi(x) = k\varphi(x) \tag{41}$$

$$Q\varphi(x) = k\chi(x). \tag{42}$$

Then we may use the phase formalism by introducing a phase variable and an envelope variable: $\varphi(x) = \mathrm{e}^{\xi(x)} \sin\vartheta(x)$ and $\chi(x) = -\mathrm{e}^{\xi(x)} \cos\vartheta(x)$. The phase variable obeys a stochastic differential equation with a noise multiplying a trigonometric function of the phase. For convenience we introduce an additive process $\zeta(x)$ defined as $\zeta(x) = \pm\frac{1}{2}\ln|\tan\vartheta(x)|$. The sign '+' is chosen for $(\vartheta \bmod \pi) \in [0, \pi/2]$ and the sign '−' for $(\vartheta \bmod \pi) \in [\pi/2, \pi]$. This new process obeys the stochastic differential equation

$$\frac{\mathrm{d}}{\mathrm{d}x}\zeta = k\cosh 2\zeta \pm \phi(x). \tag{43}$$

Between two nodes of the wavefunction, the variable ζ twice crosses the interval $]-\infty, +\infty[$. Note that when $\phi(x)$ is a white noise of zero mean, the sign $\pm$ can be disregarded. The study of the time required by the process to cross the interval can be performed by the same method as above: we introduce the 'time' $\tilde{\Lambda}(\zeta)$ needed to go from ζ to $+\infty$. The Laplace transform of the distribution $h(\alpha, \zeta) = \langle \mathrm{e}^{-\alpha\tilde{\Lambda}} \mid \zeta(0) = \zeta; \zeta(\tilde{\Lambda}) = +\infty\rangle$ obeys a diffusion equation $\left(k\cosh 2\zeta\ \partial_\zeta + \frac{g}{2}\partial_\zeta^2\right)h(\alpha, \zeta) = \alpha h(\alpha, \zeta)$ that involves the backward Fokker–Planck operator related to the Langevin equation (43).

In the low-energy limit $k \ll g$ we expect that most of the 'time' $\Lambda \equiv \tilde{\Lambda}(-\infty)$ is spent in the region where the potential is almost flat (see figure 4), therefore we replace the diffusion equation for $h(\alpha, \zeta)$ by the free diffusion equation $\frac{g}{2}\partial_\zeta^2 h(\alpha, \zeta) = \alpha h(\alpha, \zeta)$ on the finite interval

[31] A more complete picture of the properties of this model at $E = 0$ is given in several works: (A) moments and correlations of the zero mode are studied in [66,194]. (B) Additionally to the statistical properties of the time delay, equation (27), (C) the distribution of the transmission probability is derived in [198]. In particular it was shown that the average transmission through an interval of length L decreases like $\langle T\rangle \propto 1/\sqrt{L}$, which is slower than in the diffusive regime. (D) The existence of a finite conductivity was demonstrated in [111].

$\zeta \in [\zeta_-, \zeta_+]$, with a reflecting boundary condition at one side $\partial_\zeta h(\alpha, \zeta_-) = 0$ and $h(\alpha, \zeta_+) = 1$ at the other side (which corresponds actually to the absorption at $\zeta = \zeta_+$). The coordinates $\zeta_\pm$ are the points where the deterministic force and the white noise have equal strengths.

Now, we can obtain $h(\alpha, \zeta)$ straightforwardly,

$$\langle \mathrm{e}^{-\alpha\Lambda} \rangle \simeq h(\alpha, \zeta_-) = \frac{1}{\cosh \sqrt{\alpha/N(E)}}, \tag{44}$$

where $N(E) = g/2 \ln^2(g/k)$ is the IDoS per unit length.

If $\Lambda \equiv \tilde{\Lambda}(-\infty)$ is the 'time' needed to cross the interval, the distance between two nodes of the wavefunction is a sum of two such (independent) random variables $\ell = \Lambda_1 + \Lambda_2$. Therefore its distribution is given by inverse Laplace transformation of $\langle \mathrm{e}^{-\alpha\ell} \rangle = 1/\cosh^2 \sqrt{\alpha/N(E)}$. We obtain

$$P(\ell) = N(E)\varpi_0(N(E)\ell), \tag{45}$$

where $\varpi_0(x)$ is the inverse Laplace transform of $\cosh^{-2} \sqrt{s}$:

$$\varpi_0(x) = \Upsilon(x) \sum_{m=0}^{\infty} [\pi^2(2m+1)^2 x - 2] \, \mathrm{e}^{-\frac{\pi^2}{4}(2m+1)^2 x} \underset{x\to\infty}{\simeq} \pi^2 x \, \mathrm{e}^{-\frac{\pi^2}{4}x} \tag{46}$$

$$= \frac{4}{\sqrt{\pi}} \frac{\Upsilon(x)}{x^{3/2}} \sum_{m=1}^{\infty} (-1)^{m+1} m^2 \, \mathrm{e}^{-m^2/x} \underset{x\to 0}{\simeq} \frac{4}{\sqrt{\pi}} \frac{\Upsilon(x)}{x^{3/2}} \, \mathrm{e}^{-1/x}, \tag{47}$$

where $\Upsilon(x)$ is the Heaviside function.

We find the distribution of the ground-state energy:

$$W_0(E) = L\rho(E)\varpi_0(LN(E)), \tag{48}$$

with the following limiting behaviour:

$$W_0(E) \simeq \frac{8}{\sqrt{2\pi g L}} \frac{1}{E} \exp - \frac{\ln^2(g^2/E)}{2gL} \qquad \text{for} \quad E \ll g^2 \, \mathrm{e}^{-\sqrt{2gL}} \tag{49}$$

$$\simeq \frac{8\pi^2 g^2 L^2}{E \ln^5(g^2/E)} \exp - \frac{\pi^2 g L}{2 \ln^2(g^2/E)} \qquad \text{for} \quad g^2 \, \mathrm{e}^{-\sqrt{2gL}} \ll E \ll g^2. \tag{50}$$

In [204], an integral representation of $W_n(E)$ is also given together with an explicit expression for $W_1(E)$.

It is also interesting to point out that the ground-state distribution is characterized by a typical value $E_0^{\mathrm{typ}} \simeq g^2 \, \mathrm{e}^{-gL}$, a median value $E_0^{\mathrm{med}} \sim g^2 \, \mathrm{e}^{-\sqrt{gL}}$, and a mean value $\langle E_0 \rangle \sim g^2 (gL)^{1/2} \, \mathrm{e}^{-C(gL)^{1/3}}$ where C is a numerical constant (see [204]). This latter expression has also been obtained in [171] where upper and lower bounds were found using a perturbative expression for the ground-state energy as a functional of $\phi(x)$.

The distribution (46) was obtained in [150] in the context of the classical diffusion by using a real space renormalization group method. In this case the distribution is interpreted as the distribution of the smallest relaxation time.

In summary, these two examples illustrate the fact that extreme value spectral statistics provides an information on correlations of eigenvalues: the extreme value statistics of independent and identically distributed random variables have been classified by Gumbel [120]. Therefore extreme value distribution for eigenvalues that differ from one of the three Gumbel's laws indicates level correlations.

5. Trace formulae, spectral determinant and diffusion on graphs

5.1. Introduction

Up to now we have discussed several questions related to the physics of weak and strong localization. In the previous section we have considered spectral properties while in sections 2 and 3 we mostly discussed transport properties.

In the present section we are going to review several results related to the study of the Laplace operator on metric graphs. An object at the core of our discussion is the spectral determinant of the Laplace operator, formally defined as $S(\gamma) = \det(\gamma - \Delta)$, where γ is a spectral parameter. This quantity encodes the information on the spectrum of the Laplace operator on the graph. Subsection 5.2 recalls the basic conventions required to describe metric graphs. Subsections 5.3 and 5.4 review general results on trace formulae and spectral determinants. These subsections will appear at first sight quite technical and unrelated to the previous sections. However we will see that there exists a close relation with the question of quantum transport: the Laplace operator is the generator of the diffusion on the graph and its spectral properties play a central role in the study of transport. This connection, already evoked in the introduction and section 2, will be emphasized again in subsection 5.6 where the explicit relation between quantum transport and spectral determinant is recalled.

One interest for spectral determinants is that they can be used as generating functions for various quantities characterizing the diffusion on the graph. This will be illustrated by using the connection with trace formulae (section 5.3) and further exploited in subsection 5.6 in the context of quantum transport. The efficiency of the method stems from the fact that, even though $S(\gamma)$ seems to be a complicated object at first sight, involving an infinite number of eigenvalues, it can be expressed as the determinant of a finite size matrix. This relation, established by Pascaud and Montambaux [177, 178], allows computing easily and systematically the spectral determinant for arbitrary graphs.

The study of the Laplace operator on metric graphs (or *quantum graphs*) is not restricted to transport and appears in many physical contexts ranging from organic molecules [187], superconducting networks [6], phase coherent transport in networks of weakly disordered wires [3, 81, 178, 210], transport in mesoscopic networks [20, 52, 106, 191, 192, 209, 218] or metallic agregates [53]. We are not going to review this history and refer the interested reader to [3, 6, 19, 59, 141, 143] (for a recent review see the appendix of Pavel Exner in [5]). Mathematical aspects of quantum graphs are discussed in the recent issues of *Waves Random Media* **14** (2004) and *J. Phys. A: Math. Gen.* **38** (22) (June 2005). See in particular [146, 147].

5.2. Description of metric graphs

We collect some background material from the theory of graphs and establish our notations and conventions (illustrated in figure 5).

Vertices, bonds, arcs. Let us consider a network of B wires (bonds) connected at V vertices. The latter are labelled with Greek indices $\alpha, \beta, \ldots$. Therefore, the bonds of the graph can be denoted by a couple of Greek indices $(\alpha\beta)$. The oriented bonds, denoted as *arcs*, will also play an important role. The two arcs related to the bond $(\alpha\beta)$ will be labelled by $\alpha\beta$ and $\beta\alpha$ or more simply with Roman letters $i, j, \ldots$.

Adjacency matrix. The basic object is the adjacency $V \times V$ matrix $a_{\alpha\beta}$ characterizing the topology of the network: $a_{\alpha\beta} = 1$ if α and β are connected by a bond; $a_{\alpha\beta} = 0$

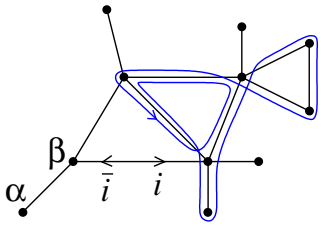

Figure 5. An example of graph with 11 vertices and 13 bonds. The arrows show the orientations of the arc i and the reversed arc $\bar{i}$. The blue curve is an example of (primitive) orbit with one backtracking.

otherwise[32]. The connectivity of the vertex α, denoted by m_α, is related to the adjacency matrix by $m_\alpha = \sum_\beta a_{\alpha\beta}$. Summed over the remaining index, the adjacency matrix gives the number of arcs: $\sum_{\alpha,\beta} a_{\alpha\beta} = 2B$.

Orbits. A path is an ordered set of arcs such that the end of an arc coincides with the beginning of the following arc. The equivalence class of all closed paths equivalent by cyclic permutations is called an *orbit*. An orbit is said to be *primitive* when it cannot be decomposed as a repetition of a shorter orbit.

Scalar functions. The graphs we consider here are not simply topological objects but have also some metric properties: the bond $(\alpha\beta)$ is characterized by its length $l_{\alpha\beta}$ and identified with the interval $[0, l_{\alpha\beta}]$ of $\mathbb{R}$. A scalar function $\psi(x)$ is defined by its components $\varphi_{\alpha\beta}(x_{\alpha\beta})$ on each bond, where $x_{\alpha\beta}$ is the coordinate measuring the distance along the bond from the vertex α (note that $x_{\alpha\beta} + x_{\beta\alpha} = l_{\alpha\beta}$).

Continuous boundary conditions. When studying the Laplace operator Δ acting on scalar functions, boundary conditions at the vertices must be specified in order to ensure self-adjointness of the operator. Let us introduce the notations:

$$\varphi_{\alpha\beta} \equiv \varphi_{\alpha\beta}(x_{\alpha\beta} = 0) \tag{51}$$

$$\varphi'_{\alpha\beta} \equiv \frac{\mathrm{d}\varphi_{\alpha\beta}}{\mathrm{d}x_{\alpha\beta}}(x_{\alpha\beta} = 0), \tag{52}$$

for the value of the function and its derivative at the vertex α, along the arc $\alpha\beta$. The continuous boundary conditions assume

(i) Continuity of the function at each vertex: all the components $\varphi_{\alpha\beta}$ for all β neighbours of α are equal. The value of the function at the vertex is denoted by $\varphi(\alpha)$.

(ii) $\sum_\beta a_{\alpha\beta}\varphi'_{\alpha\beta} = \lambda_\alpha\varphi(\alpha)$ where the adjacency matrix in the sum constrains it to run over the neighbouring vertices of α. Therefore the sum runs over all wires issuing from the vertex. The real parameter λ_α allows describing several boundary conditions: $\lambda_\alpha = \infty$ enforces the function to vanish, $\varphi(\alpha) = 0$, and corresponds to the Dirichlet boundary condition. $\lambda_\alpha = 0$ corresponds to the Neumann boundary condition. We refer to the case

[32] Note that this definition assumes that two vertices are connected by at most one bond and that a bond never forms a loop. We emphasize that *this does not imply any particular restriction on the topology of the graph*: one can always introduce a vertex on a bond, which separates the bond into two bonds, without modifying the properties of the graph. The numbers of vertices and bonds can always be made arbitrary large and this is partly a matter of choice. The case of closed bonds (forming a loop) or vertices connected by multiple bonds requires a simple generalization of the formalism presented here (see for example [177] and appendix C of [3]). This generalization allows us in particular to minimize B and V, which makes the computation sometimes easier.

of a finite λ_α as 'mixed boundary conditions'. In the problem of classical diffusion, the Dirichlet condition describes the connection to a reservoir that absorbs particles, while the Neumann condition ensures conservation of the probability current and describes an internal vertex.

General boundary conditions. Thanks to the continuity hypothesis, the simple boundary conditions we have just described allow us to introduce vertex variables $\varphi(\alpha)$ (this is convenient since the number of vertices V is usually smaller than the number of arcs $2B$). However these are not the most general boundary conditions, and in general the different components associated with the arcs issuing from a given vertex do not have *a priori* the same limit at the vertex. The most general boundary conditions can be written as

$$C\varphi + D\varphi' = 0 \tag{53}$$

where φ and φ' are the column vectors of dimension $2B$ collecting variables (51) and (52), respectively. C and D are two square $2B \times 2B$ matrices. In the arc formulation, the information on the topology of the graph is encoded in these two matrices. The self-adjointness of the Laplace operator is ensured if these two matrices satisfy the following conditions [139]: (i) $CD^\dagger$ is self-adjoint. (ii) The $2B \times 4B$ matrix (C, D) must have maximal rank. Note that the choice of C and D is not unique. The introduction of boundary conditions without continuity at the vertices has been motivated physically in [18, 52, 89, 90, 106, 192].

Scattering theory interpretation. We can give a more clear physical meaning to these conditions in a scattering setting. Let us consider the equation $-\Delta\varphi(x) = E\varphi(x)$ for a positive energy $E = k^2$. We decompose the component on the bond as the superposition of an incoming and an outgoing plane wave: $\varphi_{\alpha\beta}(x_{\alpha\beta}) = I_{\alpha\beta}\,\mathrm{e}^{-\mathrm{i}kx_{\alpha\beta}} + O_{\alpha\beta}\,\mathrm{e}^{\mathrm{i}kx_{\alpha\beta}}$. It is convenient to collect the amplitudes in column vectors I and O. The vector I contains the incoming plane wave amplitudes and the vector O the outgoing plane wave amplitudes. Both are related by a vertex scattering matrix: $O = QI$. The self-adjointness of the Schrödinger operator is now ensured by imposing the unitarity of the scattering matrix: $Q^\dagger Q = 1$. The relation between the two formulations yields

$$Q = (\sqrt{\gamma}D - C)^{-1}(\sqrt{\gamma}D + C). \tag{54}$$

For the discussion below it is convenient to introduce the parameter γ related to the energy by $E = -\gamma = k^2 + \mathrm{i}0^+$ (the matrix Q is unitary for $E > 0$ only). An example of a matrix Q for one vertex without continuity of the wavefunction was given in [52, 106, 192]. This particular choice has become popular in mesoscopic physics (see also [209] where a more convenient parametrization was provided).

Since we are considering here compact graphs, we are dealing only with discrete spectrum. The study of noncompact graphs (with some wires of infinite length), which have continuous spectra, requires a scattering theory approach, initiated by the work of Shapiro [191, 192] and discussed in [2, 20, 25, 108, 139, 142, 143, 205, 206, 208, 209].

Magnetic fluxes. The Laplace operator arises in the context of diffusion equation but also in quantum mechanics. In this last case a natural generalization is to introduce a magnetic field. This is achieved by introducing a 1-form $A(x)\,\mathrm{d}x$ along the wires (the derivative must then be replaced by a covariant derivative: $\mathrm{d}_x \to \mathrm{D}_x = \mathrm{d}_x - \mathrm{i}A(x)$). We denote by $\theta_{\alpha\beta} = \int_\alpha^\beta \mathrm{d}x\,A(x)$ the corresponding line integral along the arc $\alpha\beta$. In the context of classical diffusion, magnetic fluxes and winding numbers are conjugated variables.

5.3. Trace formulae and zeta functions

Trace formulae play an important role in spectral theory. A famous example is the Selberg trace formula which may be viewed as an extension of the Poisson summation formula to non-commutative groups [190]. An analogous formula in physics is the Gutzwiller trace formula [123] that has extensively been used in the context of quantum chaos and mesoscopic physics. Although one is exact and the other only a semiclassical approximation, both of them express the partition function (or the density of states, whose Laplace transform gives the partition function) as a sum over closed geodesics. They provide a connection between quantum properties (spectrum) and classical properties (classical trajectories). Below we discuss two examples of exact trace formulae that have been derived for graphs and their relation to spectral determinants.

5.3.1. Roth's trace formula. It expresses the trace of the heat kernel (partition function $Z(t) = \mathrm{Tr}\{\mathrm{e}^{t\Delta}\}$) as an infinite series of contributions of periodic orbits on the graph. This remarkable formula, due to Roth [185, 186], applies to graphs with continuous boundary conditions with $\lambda_\alpha = 0$. It it easy to include magnetic fluxes additionally:

$$Z(t) = \frac{\mathcal{L}}{2\sqrt{\pi t}} + \frac{V-B}{2} + \frac{1}{2\sqrt{\pi t}} \sum_{\mathcal{C}} l(\widetilde{\mathcal{C}})\alpha(\mathcal{C})\, \mathrm{e}^{-\frac{l(\mathcal{C})^2}{4t} + \mathrm{i}\theta(\mathcal{C})}, \tag{55}$$

where $\mathcal{L}$ is the 'volume' of the graph, i.e. the total length $\mathcal{L} = \sum_{(\alpha\beta)} l_{\alpha\beta}$. The sum runs over all orbits $\mathcal{C} = (i_1, i_2, \ldots, i_n)$ constructed in the graph. $l(\mathcal{C}) = l_{i_1} + \cdots + l_{i_n}$ is the total length of the orbit, and $\theta(\mathcal{C})$ the magnetic flux enclosed by it. $\widetilde{\mathcal{C}}$ designates the primitive orbit associated with a given orbit $\mathcal{C}$. The weight $\alpha(\mathcal{C})$ depends on the connectivity of the vertices visited by the orbit: $\alpha(\mathcal{C}) = \epsilon_{i_1 i_2}\epsilon_{i_2 i_3}\cdots\epsilon_{i_n i_1}$. The matrix ϵ couples the arcs of the graph[33]:

- if i ends at vertex α and j starts from it, we have $\epsilon_{ij} = 2/m_\alpha$, where m_α is the connectivities of the vertex;
- if moreover i and $j = \bar{i}$ are the reversed arcs $\epsilon_{i\bar{i}} = 2/m_\alpha - 1$;
- otherwise $\epsilon_{ij} = 0$.

It is worth mentioning that the Roth trace formula has found recently some practical applications to analyse magnetoconductance measurements on large square networks[34] [94].

5.3.2. Ihara–Bass trace formula. Instead of considering metric graphs we now turn to graphs viewed as purely combinatorial structures consisting of vertices connected by bonds of equal lengths ($l_{\alpha\beta} = 1$). All the information is therefore encoded in the adjacency matrix A. In this setting, the Ihara ζ-function is defined as

$$\zeta(u)^{-1} = \prod_{\widetilde{\mathcal{C}}_B} (1 - u^{l(\widetilde{\mathcal{C}}_B)}), \tag{56}$$

where the infinite product extends over all primitive backtrackless orbits $\widetilde{\mathcal{C}}_B$. The Ihara–Bass trace formula relates this infinite product to the determinant of a finite size matrix [28, 197]:

$$\zeta(u)^{-1} = (1-u^2)^{B-V} \det((1-u^2)\mathbf{1} - uA + u^2 Y) \tag{57}$$

[33] Note that the parameter ϵ_{ij} has a simple interpretation in the scattering formulation [209]: it is the probability amplitude to be transmitted from arc i to arc j. The arc matrices ϵ and Q are related by $\epsilon_{ij} = Q_{i\bar{j}}$ where $\bar{j}$ denotes the reversed arc.

[34] More precisely, the expansion given below by equation (62) for the Laplace transform of the partition function is relevant in this case.

where $\mathbf{1}$ is the identity matrix, A is the adjacency matrix ($A_{\alpha\beta} \equiv a_{\alpha\beta}$) and Y is the diagonal matrix encoding all connectivities: $Y_{\alpha\beta} = \delta_{\alpha\beta} m_\alpha$. This relation was derived by Ihara [129] for regular graphs (all vertices with same connectivity) and later generalized to arbitrary graphs by Bass [28]. The formalism that we have developed for metric graphs is flexible enough to describe these combinatorial structures in the same setting. We will see below that the ζ-function is in fact directly related to the spectral determinant. Moreover the Ihara–Bass trace formula can be further generalized to include backtrackings.

5.4. *Spectral determinant*

In the physics literature spectral determinants arise in evaluating path integrals which are quadratic in the fluctuation around a given background field. A well-known technique for regularizing such quadratic path integrals is the ζ-function regularization. Given a certain operator $\mathcal{O}$ whose eigenvalues E_n are known, one defines the following ζ-function: $\zeta(s) = \sum_n E_n^{-s}$. This expression, which converges for s sufficiently large, can be analytically extended to a meromorphic function regular at the origin. The corresponding regularized determinant is then $\det \mathcal{O} = \exp(-\zeta'(0))(\equiv \prod_n E_n$ formally). One can find a general discussion on functional determinants in [96].

In the context of graphs another regularization of the determinant of the Laplace operator has been used and has proved to be directly related to several physical quantities. If we introduce the trace of the resolvent $g(\gamma) = \sum_n (\gamma + E_n)^{-1}$, the spectral determinant is defined as $S(\gamma) = \exp\left(\int^\gamma \mathrm{d}\gamma' g(\gamma')\right)$ (it can formally be written as[35] $S(\gamma) = \prod_n (\gamma + E_n)$). Moreover, the spectral parameter γ has in some cases a physical meaning (see section 5.6).

5.4.1. Laplace operator Δ with continuous boundary conditions. Pascaud and Montambaux have shown in [177, 178] that $S(\gamma) = \det(\gamma - \Delta)$ can be related to the determinant of a $V \times V$-matrix:

$$S(\gamma) = \gamma^{\frac{V-B}{2}} \prod_{(\alpha\beta)} \sinh(\sqrt{\gamma} l_{\alpha\beta}) \det M, \tag{58}$$

where the product runs over all bonds of the network. The $V \times V$-matrix M is defined as

$$M_{\alpha\beta} = \delta_{\alpha\beta} \left(\frac{\lambda_\alpha}{\sqrt{\gamma}} + \sum_\mu a_{\alpha\mu} \coth(\sqrt{\gamma} l_{\alpha\mu}) \right) - a_{\alpha\beta} \frac{\mathrm{e}^{-\mathrm{i}\theta_{\alpha\beta}}}{\sinh(\sqrt{\gamma} l_{\alpha\beta})}, \tag{59}$$

where the adjacency matrix constrains the sum to run over all vertices μ connected to α. The matrix M encodes all information about the network: topology (matrix $a_{\alpha\beta}$), lengths of the wires ($l_{\alpha\beta}$), magnetic fluxes ($\theta_{\alpha\beta}$), boundary conditions (λ_α). Below, we give several examples which show how $S(\gamma)$ is related to the characteristic function of various interesting functionals of Brownian curves on a graph.

Expression (58) was originally derived in [178] by constructing Green's function in the graph and eventually integrating it: $\int \mathrm{d}x \langle x | \frac{1}{\gamma - \Delta} | x \rangle = \frac{\partial}{\partial \gamma} \ln S(\gamma)$. A more direct derivation using path integral was later obtained in [3].

The relation between the Roth trace formula and the result (58) was addressed in [3]. The main difficulty to establish this connection is to go from vertex variables to the arc language of equation (55). A first step is to relate the determinant of the vertex-matrix, equation (58), to the determinant of an arc-matrix:

$$S(\gamma) = \gamma^{\frac{V-B}{2}} \mathrm{e}^{\sqrt{\gamma}\mathcal{L}} \det(\mathbf{1} - QR), \tag{60}$$

[35] The limit $\gamma \to 0$ of $S(\gamma)$ has been discussed in [3].

where R is the $2B \times 2B$ matrix $R_{ij} = \delta_{i\bar{j}}\, \mathrm{e}^{-\sqrt{\gamma} l_i + \mathrm{i}\theta_i}$, where $\bar{j}$ denotes the reversed arc. The matrix Q was introduced above (equation (54)) and is related to ϵ by $Q_{ij} = \epsilon_{i\bar{j}}$. For the continuous boundary conditions with $\lambda_\alpha = 0$ it is given by $Q_{ii} = 2/m_\alpha - 1$, $Q_{ij} = 2/m_\alpha$ if i and j both issue from the vertex α. $Q_{ij} = 0$ in other cases. Equation (60) holds for the most simple boundary conditions: continuous with $\lambda_\alpha = 0$. The general case is discussed below. Expanding the determinant by using $\ln \det(\mathbf{1} - QR) = -\sum_{n=1}^{\infty} \frac{1}{n} \mathrm{Tr}\{(QR)^n\}$, we eventually express the spectral determinant as an infinite product over the primitive orbits:

$$S(\gamma) = \gamma^{\frac{V-B}{2}}\, \mathrm{e}^{\sqrt{\gamma}\mathcal{L}} \prod_{\widetilde{\mathcal{C}}} (1 - \alpha(\widetilde{\mathcal{C}})\, \mathrm{e}^{-\sqrt{\gamma} l(\widetilde{\mathcal{C}}) + \mathrm{i}\theta(\widetilde{\mathcal{C}})}). \tag{61}$$

This shows that the spectral determinant is a zeta function (references on zeta functions on graphs are [57, 197]). The last step to connect this formula to Roth's trace formula is to note that

$$\frac{\partial}{\partial \gamma} \ln S(\gamma) = \frac{\mathcal{L}}{2\sqrt{\gamma}} + \frac{V-B}{2\gamma} + \frac{1}{2\sqrt{\gamma}} \sum_{\mathcal{C}} l(\widetilde{\mathcal{C}}) \alpha(\mathcal{C})\, \mathrm{e}^{-\sqrt{\gamma} l(\mathcal{C}) + \mathrm{i}\theta(\mathcal{C})}, \tag{62}$$

where the sum now runs over all orbits (if $\mathcal{C}$ is not primitive, $\widetilde{\mathcal{C}}$ designates the related primitive orbit). Finally we perform an inverse Laplace transform of this expression, $\int_0^\infty \mathrm{d}t\, Z(t)\, \mathrm{e}^{-\gamma t} = \frac{\partial}{\partial \gamma} \ln S(\gamma)$ and eventually recover equation (55). Examples of applications are studied in [3].

5.4.2. Schrödinger operator $-\Delta + V(x)$ with general boundary conditions. Result (58) of Pascaud and Montambaux has been generalized by one of us. In [72, 73] a similar formula was obtained for the spectral determinant of the Schrödinger operator $-\Delta + V(x)$ (the Hill operator), where $V(x)$ is a scalar potential defined on the graph. In [74] the formula was further extended to describe general boundary conditions as well. As an illustration we construct the generating function of the number of closed orbits with a given number of backtrackings [129, 226].

The starting point is to introduce two linearly independent solutions of the differential equation $\left(-\mathrm{d}_x^2 + V_{\alpha\beta}(x) + \gamma\right) f(x) = 0$ on $[0, l_{\alpha\beta}]$. We associate each solution with an arc. Let us denote $f_{\alpha\beta}(x_{\alpha\beta})$ the function satisfying

$$f_{\alpha\beta}(0) = 1 \qquad \text{and} \qquad f_{\alpha\beta}(l_{\alpha\beta}) = 0. \tag{63}$$

Therefore a second solution of the differential equation is naturally denoted by $f_{\beta\alpha}(x_{\beta\alpha}) = f_{\beta\alpha}(l_{\alpha\beta} - x_{\alpha\beta})$. The Wronskian of these two solutions, defined as $W_{\alpha\beta} = f_{\alpha\beta}(x_{\alpha\beta}) \frac{\mathrm{d} f_{\beta\alpha}(x_{\beta\alpha})}{\mathrm{d}x_{\alpha\beta}} - \frac{\mathrm{d} f_{\alpha\beta}(x_{\alpha\beta})}{\mathrm{d}x_{\alpha\beta}} f_{\beta\alpha}(x_{\beta\alpha})$, is constant along the bond: $W_{\alpha\beta} = W_{\beta\alpha} = -f'_{\alpha\beta}(l_{\alpha\beta}) = -f'_{\beta\alpha}(l_{\alpha\beta})$. If we consider the case $V(x) = 0$, the solution is simply $f_{\alpha\beta}(x_{\alpha\beta}) = \frac{\sinh \sqrt{\gamma}(l_{\alpha\beta} - x_{\alpha\beta})}{\sinh \sqrt{\gamma} l_{\alpha\beta}} \equiv \frac{\sinh \sqrt{\gamma} x_{\beta\alpha}}{\sinh \sqrt{\gamma} l_{\alpha\beta}}$.

All the required information about the potential is contained in the $2B \times 2B$ arc-matrix N, defined as

$$N_{\alpha\beta,\mu\eta} = \delta_{\alpha\mu}\delta_{\beta\eta} f'_{\alpha\beta}(0) - \delta_{\alpha\eta}\delta_{\beta\mu} f'_{\alpha\beta}(l_{\alpha\beta}). \tag{64}$$

This matrix couples a given arc to itself and to its reversed arc, only. If we assume that *the matrices C and D are independent on the spectral parameter γ*, it was shown in [74] that

$$S(\gamma) = \det(\gamma - \Delta + V(x)) = \prod_{(\alpha\beta)} \frac{1}{W_{\alpha\beta}} \det(C + DN) \tag{65}$$

where the product runs over all bonds. Functional determinants on a segment of $\mathbb{R}$ with general boundary conditions at the boundaries have been studied by McKane and Tarlie [164] using the formalism developed by Forman [96].

It is also interesting to encode the information on the potential $V(x)$ in the matrix R defined as[36]

$$R \equiv (\sqrt{\gamma}\mathbf{1} + N)(\sqrt{\gamma}\mathbf{1} - N)^{-1}. \tag{66}$$

Then

$$S(\gamma) = \prod_{(\alpha\beta)} \frac{1}{W_{\alpha\beta}} \frac{1}{\det(\mathbf{1}+R)} \det(C - \sqrt{\gamma}D) \det(\mathbf{1} - QR) \tag{67}$$

where the matrix $Q = (\sqrt{\gamma}D - C)^{-1}(\sqrt{\gamma}D + C)$ was defined above by equation (54). Let us explain the structure of equation (67): the term $\det(\mathbf{1} + R)\prod_{(\alpha\beta)} W_{\alpha\beta}$ contains information on the potential only[37]. The factor $\det(C - \sqrt{\gamma}D)$ contains only information on the topology of the graph. The most interesting part is the last term $\det(\mathbf{1} - QR)$ combining both informations. In particular this last part generates the infinite contributions of primitive orbits in (61).

5.4.3. Permutation–invariant boundary conditions. In the previous section the matrices describing the graph are $2B \times 2B$ arc matrices. A simplification can be brought by passing to vertex variables. In the arc formulation, C and D define the topology of the graph: two arcs coupled by C and/or D issue from the same vertex. Therefore it is possible to organize the basis of arcs in such a way that the matrices C and D have similar block diagonal structures. The matrices are made of V square blocks, each corresponding to a vertex. A given block, of dimension $m_\alpha \times m_\alpha$ and denoted by C_α (and D_α), corresponds to the m_α arcs issuing from the vertex α. If we assume that the boundary conditions are invariant under any permutation of the nearest neighbours of α, then it is possible to introduce vertex variables. In this case we can write

$$C_\alpha = c_\alpha \mathbf{1} + t_\alpha F_\alpha \tag{68}$$

$$D_\alpha = d_\alpha \mathbf{1} + w_\alpha F_\alpha \tag{69}$$

where F_α is a matrix with all its elements equal to 1. The boundary conditions at the vertex α are characterized by the four parameters c_α, d_α, t_α and w_α (note however that this choice is not unique).

Now, let us show that, for boundary conditions given by equations (68) and (69) and $V(x) \neq 0$, the spectral determinant can be expressed in terms of the vertex $V \times V$-matrix.

We proceed as before but, this time, we consider, for each bond, two other independent solutions, $\chi_{\alpha\beta}(x_{\alpha\beta})$ and $\chi_{\beta\alpha}(l_{\alpha\beta} - x_{\alpha\beta}) = \chi_{\beta\alpha}(x_{\beta\alpha})$, of the equation $\left(-\mathrm{d}^2_{x_{\alpha\beta}} + V_{\alpha\beta}(x_{\alpha\beta}) + \gamma\right)$ $\chi(x_{\alpha\beta}) = 0$ that satisfy the following conditions:

$$c_\alpha \chi_{\alpha\beta}(0) + d_\alpha \chi'_{\alpha\beta}(0) = 1 \tag{70}$$

$$c_\beta \chi_{\alpha\beta}(l_{\alpha\beta}) - d_\beta \chi'_{\alpha\beta}(l_{\alpha\beta}) = 0. \tag{71}$$

We denote by $\Xi_{\alpha\beta}$ the Wronskian of $\chi_{\alpha\beta}$ and $\chi_{\beta\alpha}$. Following the same steps as before, we get the spectral determinant (up to a multiplicative constant):

$$S(\gamma) = \prod_{(\alpha\beta)} \frac{1}{\Xi_{\alpha\beta}} \det M \tag{72}$$

[36] Let us remark that, for the free case ($V(x) \equiv 0$), we recover the expression of the matrix R given above, coupling the arc $\alpha\beta$ to the reversed arc $\beta\alpha$ only: $R_{\alpha\beta,\mu\eta} = \delta_{\alpha\eta}\delta_{\beta\mu}\, \mathrm{e}^{-\sqrt{\gamma}l_{\alpha\beta}}$.

[37] The matrix N encodes the information about the potential on the bonds through $f'_{\alpha\beta}(0)$ and $f'_{\alpha\beta}(l_{\alpha\beta})$. This information can also be introduced through transmission $t_{\alpha\beta}$ and reflection $r_{\alpha\beta}$ amplitudes by the potential $V_{\alpha\beta}(x)$. This relation is developed in [209]. It is interesting to point out that $\det(\mathbf{1} + R)\prod_{(\alpha\beta)} W_{\alpha\beta} = 2^B \gamma^{B/2} \prod_{(\alpha\beta)} t_{\alpha\beta} = 2^B \gamma^{B/2} \prod_{(\alpha\beta)} R_{\alpha\beta,\beta\alpha}$.

where M is the $V \times V$-matrix:

$$M_{\alpha\beta} = \delta_{\alpha\beta}\left(1 + \sum_{\mu} a_{\alpha\mu}[t_\alpha \chi_{\alpha\mu}(0) + w_\alpha \chi'_{\alpha\mu}(0)]\right) + a_{\alpha\beta}\,[c_\alpha w_\alpha - t_\alpha d_\alpha]\,\Xi_{\alpha\beta}. \tag{73}$$

Equation (65), expressing the determinant in terms of arc matrices, and equation (72), expressing it in terms of vertex matrix, have been derived up to multiplicative constants independent on γ. We can establish a precise relation by comparing their behaviour for $\gamma \to \infty$. We end up with

$$\prod_{(\alpha\beta)} \frac{1}{W_{\alpha\beta}} \det(C + DN) = \prod_{(\alpha\beta)} \frac{1}{\Xi_{\alpha\beta}} \det M. \tag{74}$$

5.4.4. Free case ($V(x) = 0$). Applications: counting backtrackings. In this subsection we show an application of generalized boundary conditions to count backtrackings (the figure 5 shows an orbit with one backtracking).

We now consider the case $V(x) \equiv 0$ still with permutation–invariant boundary conditions. With the notations

$$\eta_\alpha = \frac{c_\alpha + \sqrt{\gamma} d_\alpha}{c_\alpha - \sqrt{\gamma} d_\alpha}, \qquad \rho_\alpha = \frac{\mu_\alpha^- - \mu_\alpha^+}{1 + m_\alpha \mu_\alpha^-} \qquad \text{and} \qquad \mu_\alpha^\pm = \frac{t_\alpha \pm \sqrt{\gamma} w_\alpha}{c_\alpha \pm \sqrt{\gamma} d_\alpha}$$

equations (74), (66) and (54) lead to

$$\det(\mathbf{1} - QR) = 2^{-V} \prod_{\alpha} (\rho_\alpha \eta_\alpha) \prod_{(\alpha\beta)} (1 - \eta_\alpha \eta_\beta \, \mathrm{e}^{-2\sqrt{\gamma} l_{\alpha\beta}}) \det M \tag{75}$$

and the $V \times V$-matrix M takes the form

$$M_{\alpha\beta} = \delta_{\alpha\beta}\left(\frac{2}{\rho_\alpha \eta_\alpha} - \frac{m_\alpha}{\eta_\alpha} + \frac{1}{\eta_\alpha} \sum_{\mu} a_{\alpha\mu} \frac{1 + \eta_\alpha \eta_\mu \, \mathrm{e}^{-2\sqrt{\gamma} l_{\alpha\mu}}}{1 - \eta_\alpha \eta_\mu \, \mathrm{e}^{-2\sqrt{\gamma} l_{\alpha\mu}}}\right) - a_{\alpha\beta} \frac{2\,\mathrm{e}^{-\sqrt{\gamma} l_{\alpha\beta}}}{1 - \eta_\alpha \eta_\beta \, \mathrm{e}^{-2\sqrt{\gamma} l_{\alpha\beta}}}. \tag{76}$$

Note that the expression (59) is recovered for $\eta_\alpha = 1$ and $\rho_\alpha = 2/(m_\alpha + \lambda_\alpha/\sqrt{\gamma}\,)$.

For permutation-invariant boundary conditions, the matrices C, D and Q (equation (54)) are block-diagonal. The block Q_α takes the simple form,

$$Q_\alpha = \eta_\alpha(-\mathbf{1} + \rho_\alpha F_\alpha). \tag{77}$$

The only non-vanishing elements of the matrix QR are

$$(QR)_{\alpha\beta,\mu\alpha} = (\rho_\alpha \eta_\alpha - \eta_\alpha \delta_{\beta\mu}) \, \mathrm{e}^{-\sqrt{\gamma} l_{\alpha\mu}}. \tag{78}$$

We call $\rho_\alpha \eta_\alpha$ the transmission factor at vertex α and $\rho_\alpha \eta_\alpha - \eta_\alpha$ the reflection factor. By using the same expansion as above we write

$$\det(\mathbf{1} - QR) = \prod_{\widetilde{C}} (1 - \mu(\widetilde{C}) \, \mathrm{e}^{-\sqrt{\gamma} l(\widetilde{C})}), \tag{79}$$

where the product is taken over all primitive orbits $\widetilde{C}$ whose lengths are denoted by $l(\widetilde{C})$. An orbit being a succession of arcs $\ldots, \tau\alpha, \alpha\beta, \ldots$ with, in α, a reflection (if $\tau = \beta$) or a transmission (if $\tau \neq \beta$), the weight $\mu(\widetilde{C})$, in equation (79), will be the product of all the reflection—or transmission—factors along $\widetilde{C}$.

Graphs with wires of equal lengths. We consider the case of equal lengths $l_{\alpha\beta} = l$; then we can choose $\gamma = 1$ without loss of generality and introduce the notation $u \equiv \mathrm{e}^{-l}$. It is clear from equation (77) that a backtracking at vertex α brings a factor η_α into the weight $\mu(\widetilde{C})$. In

order to count backtrackings one has to choose the boundary conditions $\rho_\alpha \eta_\alpha = 1$ and $\eta_\alpha = \eta$. Equation (75) takes the simple form,

$$\prod_{\widetilde{C}_m} (1 - (1-\eta)^{n_R(\widetilde{C}_m)} u^m) = (1-\eta^2 u^2)^{B-V} \det((1-\eta^2 u^2)\mathbf{1} + \eta u^2 Y - uA) \equiv Z^{-1}, \tag{80}$$

where m is the number of arcs of the primitive orbit $\widetilde{C}_m$ and $n_R(\widetilde{C}_m)$ is the number of reflections (backtrackings) occurring along $\widetilde{C}_m$. Y is the $V \times V$-matrix $Y_{\alpha\beta} = \delta_{\alpha\beta} m_\alpha$ and A is the adjacency matrix.

Setting $\eta = 1$ implies $n_R(\widetilde{C}_m) = 0$ on the left-hand side of equation (80): we recover Ihara–Bass formula [28, 129, 197] where only primitive orbits without tails and backtrackings are kept. (Ihara [129] established this formula for a regular graph; the proof for a general graph is given in [28, 197] using a direct counting technique).

Now, let us consider closed random walks with a given number of backtrackings.

Equation (80) provides a non-trivial generalization of the Ihara–Bass formula (an independent derivation is also given in [26]). As an application let us consider the problem of enumerating m-steps random walks with p-backtracking steps [226]. Taking Z in (80), we get

$$u \frac{\mathrm{d} \ln Z}{\mathrm{d}u} = \sum_{m=2}^{\infty} \sum_{p=0}^{m} \sum_{\alpha=1}^{V} N_m^p(\alpha) (1-\eta)^p u^m \tag{81}$$

where $N_m^p(\alpha)$ is the number of m-steps closed random walks on the graph starting at α, with p backtrackings.

Example (the complete graph)**.** For the complete graph[38] K_V, we get the results:

$$\begin{aligned} N_2^0(\alpha) &= 0 \\ N_3^0(\alpha) &= (V-1)(V-2) \\ N_4^0(\alpha) &= (V-1)(V-2)(V-3) \\ N_5^0(\alpha) &= (V-1)(V-2)(V-3)(V-4) \\ N_6^0(\alpha) &= (V-1)(V-2)(V^3 - 9V^2 + 29V - 32). \end{aligned} \tag{82}$$

and also

$$\begin{aligned} N_2^1(\alpha) &= N_3^1(\alpha) = N_4^1(\alpha) = 0 \\ N_5^1(\alpha) &= 5(V-1)(V-2)(V-3) \\ N_6^1(\alpha) &= 6(V-1)(V-2)(V-3)^2. \end{aligned} \tag{83}$$

Note that these expressions have been obtained when all vertices are characterized by the same parameter η. Introducing different parameters η_α allows counting of the backtrackings at a given vertex.

5.5. Quantum chaos on metric graphs

It has been recently realized that metric graphs are interesting models for quantum chaos. The paper of Kottos and Smilansky [140] has stimulated several works on spectral statistics and level correlations [24, 141, 201], and renewed the interest in the Roth trace formula [186]. Progress in the understanding of universality of spectral statistics for generic quantum graphs

[38] The complete graph K_V with V vertices is the $V-1$-simplex: each vertex is connected to all other vertices (see figure 6).

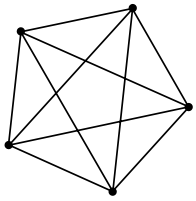

Figure 6. The complete graph K_5 (the 4-simplex): all vertices are connected to each other by bonds of equal lengths.

has been achieved by Gnutzmann and Altland [110]. One of the input of this work is the observation that the spectral average for a given graph with incommensurate bond lengths is equivalent to an average over a certain ensemble of unitarity matrices. Star graphs [36, 136] have provided simple examples of systems with intermediate level statistics similar to that observed in Šeba billiards and a precise connection has been established in [35]. There is however an interesting class of graphs which do not enter in this category [202]. Chaotic scattering and transport properties in open graphs (with some infinitely long wires) have also been studied in [25, 142, 143]. Since quantum chaos is not the central subject of our review, this list of papers is not exhaustive: we refer the reader interested in this topic to the review papers [141, 143, 202] and the PhD thesis [225].

5.6. Weak localization and Brownian motion on graphs

Our initial physical motivation for the study of the spectral determinant on graphs was based on the observation that the weak localization correction to the conductivity is directly expressed in terms of the spectral determinant. We see from equation (2) that

$$\langle \Delta\sigma \rangle = -\frac{2e^2}{\pi \,\mathrm{Volume}} \frac{\partial}{\partial \gamma} \ln S(\gamma), \tag{84}$$

where the spectral parameter is related to the phase coherence length $\gamma = 1/L_\varphi^2$. Expressions (84), (58) and (59), due to Pascaud and Montambaux [3, 177, 178], improve the approach initiated by Douçot and Rammal [81, 82].

5.6.1. Nonlocality of the quantum transport in arbitrary networks. We must stress that formula (84) corresponds to a uniform integration of the cooperon, defined as $P_c(x, x) = \langle x|\frac{1}{\gamma-\Delta}|x\rangle$, on the graph $\langle \Delta\sigma \rangle \propto -\int \mathrm{d}x\, P_c(x, x)$. This approach is limited to the case of regular graphs, where all wires play the same role. In other terms, for a nonregular network, the quantity (84) does not correspond to a quantity measured in a transport experiment. For arbitrary networks, the cooperon must be integrated over the network with appropriate non-trivial weights that depend on the topology of the whole network and the way it is connected to external contacts. Such a generalization was provided in [210].

5.6.2. Windings in a loop connected to a network. As we have mentioned in section 2.2, magnetoconductance oscillations due to a magnetic flux and winding properties are closely related. For example, if we consider an isolated ring of perimeter L pierced by a magnetic flux ϕ, the well-known behaviour of the harmonics,

$$\langle \Delta\sigma_n \rangle = \int_0^{2\pi} \frac{\mathrm{d}\theta}{2\pi} \langle \Delta\sigma(\theta) \rangle \, \mathrm{e}^{-\mathrm{i}n\theta} \propto \mathrm{e}^{-|n|L/L_\varphi}, \tag{85}$$

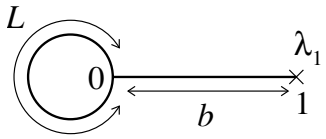

Figure 7. A diffusive ring attached to a long arm. The parameter λ_1 describes the boundary condition at vertex 1: $\lambda_1 = \infty$ for the Dirichlet boundary and $\lambda_1 = 0$ for the Neumann boundary condition.

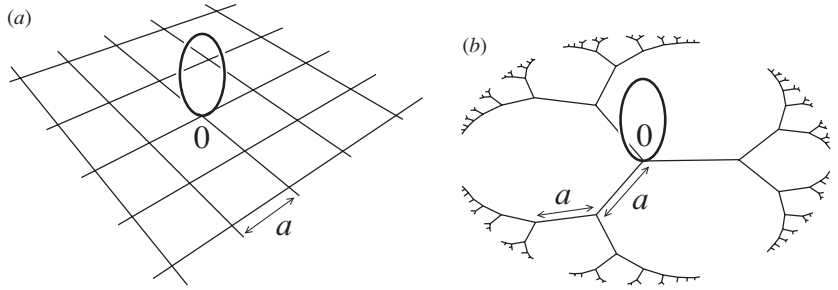

Figure 8. A diffusive ring attached to (*a*) an infinite square lattice, (*b*) an infinite Bethe lattice of connectivity $z = 3$. To ensure that the Bethe lattice is regular, it must be embedded in a constant negative curvature surface.

is a direct consequence of the fact that the winding around the ring scales with time as $n_t \propto t^{1/2}$ (normal diffusion). $\theta = 4\pi\phi/\phi_0$ is the reduced flux and $\gamma = 1/L_\varphi^2$. This effect was predicted by Al'tshuler, Aronov and Spivak (AAS) in [10] and observed in experiments on cylinder films [11, 193].

Recently it has been noted that the fact that the ring is connected to arms, which is necessary to perform a transport experiment, can strongly affect the harmonics. If we consider a ring connected to N_a long arms, in the limit $L_\varphi \ll L$, the harmonics are still given by the AAS behaviour (85), however when the perimeter is smaller than L_φ, the harmonics behave as $\langle \Delta\sigma_n \rangle \propto \mathrm{e}^{-|n|\sqrt{N_a L/L_\varphi}}$. To clarify the origin of this behaviour, the winding of Brownian trajectories around a ring connected to another network has been recently examined in [212]. This analysis is based on the fact that the winding number distribution can be expressed in terms of the spectral determinant. Let us briefly describe this approach.

We consider a ring to which is attached an arbitrary network at vertex 0 (figures 7 and 8 give examples of such a situation). Our aim is to understand how the winding around the ring is affected by the presence of the network. To answer this question we introduce the probability to start from a point x on the graph and come back to it after a time t, conditioned to wind n times around the loop:

$$\mathcal{P}_n(x, t|x, 0) = \int_{x(0)=x}^{x(t)=x} \mathcal{D}x(\tau)\, \mathrm{e}^{-\frac{1}{4}\int_0^t \mathrm{d}\tau \dot{x}(\tau)^2} \delta_{n,\mathcal{N}[x(\tau)]} \tag{86}$$

where $\mathcal{N}[x(\tau)]$ is the winding number of the path $x(\tau)$ around the loop. For simplicity, we consider the case where the initial point is the vertex 0. The computation of $\mathcal{P}_n(0, t|0, 0)$ requires some local information (the eigenfunctions of the Laplace operator at point $x = 0$). On the other hand the spectral determinant encodes a global information since it results from a spatial integration of Green's function of the Laplace operator over the network. However we have shown in [212] that if we consider mixed boundary conditions at vertex 0 described

by a parameter λ_0 (see the definition of the boundary conditions given above), we can extract the probability of interest[39] as follows:

$$\int_0^\infty \mathrm{d}t\, \mathcal{P}_n(0,t|0,0)\, \mathrm{e}^{-\gamma t} = \int_0^{2\pi} \frac{\mathrm{d}\theta}{2\pi}\, \mathrm{e}^{-\mathrm{i}n\theta}\, \frac{\mathrm{d}}{\mathrm{d}\lambda_0} \ln S^{(\lambda_0)}(\gamma)\Big|_{\lambda_0=0}, \tag{87}$$

where $S^{(\lambda_0)}(\gamma)$ is the spectral determinant for mixed boundary condition at vertex 0 and with a magnetic flux θ piercing the ring. This formula allows us to express the probability as

$$\int_0^\infty \mathrm{d}t\, \mathcal{P}_n(0,t|0,0)\, \mathrm{e}^{-\gamma t} = \frac{1}{2\sqrt{\gamma}} \frac{\sinh \sqrt{\gamma} L}{\sinh \sqrt{\gamma} L_{\mathrm{eff}}(\gamma)}\, \mathrm{e}^{-|n|\sqrt{\gamma} L_{\mathrm{eff}}(\gamma)}, \tag{88}$$

where all the information about the nature of the network attached to the ring is contained in the effective perimeter $L_{\mathrm{eff}}(\gamma)$, defined as

$$\cosh \sqrt{\gamma} L_{\mathrm{eff}}(\gamma) = \cosh \sqrt{\gamma} L + \frac{\sinh \sqrt{\gamma} L}{2\left(M_{\mathrm{net}}^{-1}\right)_{00}}. \tag{89}$$

The matrix M_{net} describes the network in the absence of the loop (it is given by equation (59); for the network of figure 8(*a*), M_{net} describes the infinite square network without the ring). The matrix element $\left(M_{\mathrm{net}}^{-1}\right)_{00}$ has a clear meaning: it is the Green function of the Laplace operator in the network (without the loop) computed at the position where the ring is attached: $\sqrt{\gamma}\left(M_{\mathrm{net}}^{-1}\right)_{00} = \langle 0|\frac{1}{\gamma-\Delta}|0\rangle$.

The effective perimeter $L_{\mathrm{eff}}(\gamma)$ probes the winding at time scale $t \sim 1/\gamma$: precisely, the winding number scales with time as $n_t \sim \sqrt{t}/L_{\mathrm{eff}}(1/t)$.

Two interesting examples are

- *Ring attached to an infinite wire (figure 7).* When a wire of length b with the Dirichlet boundary at one end is attached to the ring, it is easy to see that equation (59) gives $\left(M_{\mathrm{net}}^{-1}\right)_{00} = \tanh \sqrt{\gamma} b \underset{b\to\infty}{\longrightarrow} 1$. At large time $t \gg L^2$, the effective perimeter behaves as $L_{\mathrm{eff}} \simeq \sqrt{L}\gamma^{-1/4}$. This behaviour is related to a scaling of the winding number with time

$$n_t \propto t^{1/4}. \tag{90}$$

  The full distribution for the winding number n is given in [212]. The exponent $1/4$ that characterizes anomalously slow winding around the loop originates from the fact that the diffusive trajectory spends a long time in the infinite wire, which increases the effective perimeter at such time scales. This problem is also related to the anomalous diffusion along the skeleton of a comb, studied in [22, 222] by different methods. It is interesting to use this picture. Let us consider a random walk along the sites of a line where the diffusive particle is trapped during a time τ on each site. The trapping time is distributed according to a broad distribution $P_1(\tau) \propto \tau^{-1-\mu}$ with $0 < \mu < 1$. It follows that the distance scales with time as $n_t \sim t^{\mu/2}$ [43]. If we go back to the problem of diffusion along the skeleton of a comb (or the winding in the ring connected to the long arm), the arm plays the role of the trap. The distribution of the trapping time is given by the first return probability of the one-dimensional diffusion: $P_1(\tau) \propto \tau^{-3/2}$ and we recover equation (90).

[39] The fact that some 'local' information, such as $\mathcal{P}_n(0,t|0,0)$, can be extracted from a more 'global' object, such as the spectral determinant, by introducing the mixed boundary conditions with parameter λ_0 has been also used in the context of scattering theory in graphs in [206, 208]. The derivative in equation (87) can be understood as a functional derivative since λ_0 plays a role similar to the weight of a δ-potential at x_0. The use of functional derivatives in scattering theory for mesoscopic systems has been fruitfully used by Büttiker and co-workers (see [51] and references therein).

- *Ring attached to a square network (figure 8(a)).* When studying the winding around the loop, it is important to know whether the Brownian motion inside the network attached to the ring is recurrent or not. Let us consider the case where the network attached is a d-dimensional hypercubic network. For $d > 2$ the Brownian motion is known to be transient where as, for $d = 2$ it is neighbourhood recurrent (in $d = 1$ the Brownian motion is pointwise recurrent). Therefore we expect the dimension 2 to play a special role. In the large time limit, when $t \gg L^2$ and $t \gg a^2$ (a is the lattice spacing), we find an effective length $\sqrt{\gamma} L_{\text{eff}} \simeq \sqrt{\frac{2\pi L}{a \ln(4/\sqrt{\gamma} a)}}$, that corresponds to a scaling of the winding around the loop

$$n_t \propto (\ln t)^{1/2}. \tag{91}$$

This result can be obtained in the same way as for the ring connected to the arm. This time the plane acts as a trap. The distribution of the trapping time is given by the first return probability on a square lattice, which is known to behave at large times like $P_1(\tau) \propto 1/(\tau \ln^2 \tau)$ [27], from which we can recover equation (91).

5.6.3. Occupation time and local time distribution on a graph. Another set of problems concern occupation times, i.e., time spent by a Brownian particle in a given region. An example of such a problem is provided by the famous arc-sine law for 1d Brownian motion that gives the distribution of the time spent by a Brownian motion $(x(\tau), 0 \leqslant \tau \leqslant t | x(0) = 0)$ on the half line $\mathbb{R}^+$. This result was derived long ago by P Lévy [155]. It has been extended by Barlow, Pitman and Yor [23] for a particular graph (star graph with arms of infinite lengths): instead of an infinite line, these authors consider n semi-infinite lines originating from the same point and study the joint distribution of the times spent on each branch. More recently, this problem has been reconsidered in the case of arbitrary graphs [75]. It may be stated as follows: consider a Brownian motion $x(\tau)$ on a graph, starting from a point x_0 at time 0 and arriving at a point x_1 at time t. Let $T_{\alpha\beta}$ denotes the time spent on the wire $(\alpha\beta)$. This functional is defined as $T_{\alpha\beta}[x(\tau)] = \int_0^t \mathrm{d}\tau \theta_{\alpha\beta}(x(\tau))$ where the function $\theta_{\alpha\beta}(x)$ is 1 for $x \in (\alpha\beta)$ and 0 otherwise. Our aim is to compute the Laplace transforms of the joint distribution

$$\langle \mathrm{e}^{-\sum_{(\alpha\beta)} \xi_{\alpha\beta} T_{\alpha\beta}} \rangle = \int \mathrm{d}x_1 \mathcal{F}(x_1, x_0; t; \{\xi_{\alpha\beta}\}) \tag{92}$$

with

$$\mathcal{F}(x_1, x_0; t; \{\xi_{\alpha\beta}\}) = \int_{x(0)=x_0}^{x(t)=x_1} \mathcal{D}x(\tau)\, \mathrm{e}^{-\frac{1}{4}\int_0^t \mathrm{d}\tau \dot{x}^2 - \sum_{(\alpha\beta)} \xi_{\alpha\beta} T_{\alpha\beta}[x(\tau)]}. \tag{93}$$

Definition (92) takes into account averaging over the final point x_1. A conjugate parameter $\xi_{\alpha\beta}$ is introduced for each variable $T_{\alpha\beta}$, i.e. each bond. A closed expression of the Laplace transform of the joint distribution (92) has been derived in [75]. The result is given as a ratio of two determinants, an expression reminiscent of that of Leuridan [154], although the connection is not completely clear.

Similar methods have been also applied in [60] to study the distribution of the local time $T_{x_0}[x(\tau)] = \int_0^t \mathrm{d}\tau \delta(x(\tau) - x_0)$.

A simplification occurs when the final point coincides with the initial point. Then it is possible to relate the characteristic function to a single spectral determinant. We do not develop the general theory here but instead consider an example close to that studied in the previous subsection. Let us consider the graph in figure 7 and ask the following question: for a Brownian motion starting from x_0 at time 0 and coming back to it at time t, what is

the distribution of the time $T_{\rm arm}[x(\tau)]$ spent in the arm if in addition the Brownian motion is constrained to turn n times around the ring? It is natural to introduce the following function:

$$\mathcal{F}_n(x_0, x_0; t, \xi) = \int_{x(0)=x_0}^{x(t)=x_0} \mathcal{D}x(\tau) \exp\left(-\int_0^t \mathrm{d}\tau \left(\frac{1}{4}\dot{x}^2 + \xi\theta_{\rm arm}(x)\right)\right) \delta_{n,\mathcal{N}[x(\tau)]} \tag{94}$$

where $\mathcal{N}[x(\tau)]$ is the winding number around the ring. This function is related to the Laplace transform of the distribution of the functional $T_{\rm arm}[x(\tau)]$

$$\langle \mathrm{e}^{-\xi T_{\rm arm}[x]}\rangle_{\mathcal{C}_n} = \frac{\mathcal{F}_n(x_0, x_0; t, \xi)}{\mathcal{F}_n(x_0, x_0; t, 0)}, \tag{95}$$

where $\langle\cdots\rangle_{\mathcal{C}_n}$ denotes averaging over curves of winding n. The denominator ensures normalization. The Laplace transform of (94) is given by a relation similar to equation (87)

$$\int_0^\infty \mathrm{d}t\, \mathcal{F}_n(x_0, x_0; t, \xi)\, \mathrm{e}^{-\gamma t} = \int_0^{2\pi} \frac{\mathrm{d}\theta}{2\pi}\, \mathrm{e}^{-\mathrm{i}n\theta}\, \frac{\mathrm{d}}{\mathrm{d}\lambda_0} \ln S^{(\lambda_0)}(\gamma)\Big|_{\lambda_0=0} \tag{96}$$

where the appropriate spectral determinant is built as follows: (i) since the starting point is fixed at 0, we introduce mixed boundary conditions at this point, with a parameter λ_0 that will be used to extract the 'local information'. (ii) A magnetic flux θ is introduced (conjugate to the winding number). (iii) The spectral parameter is shifted in the arm as $\gamma \to \gamma + \xi$ to introduce the variable ξ conjugate to the time $T_{\rm arm}$.

We choose the vertex 0 as initial condition and impose the Dirichlet boundary condition (which is achieved by setting $\lambda_1 = \infty$) at the end of the arm of length b. The spectral determinant is found straightforwardly (for an efficient calculation of $S(\gamma)$ for a graph with loops, see [177] or appendix C of [3]):

$$S^{(\lambda_0)}(\gamma) = \frac{\sinh\sqrt{\gamma}L \sinh\sqrt{\gamma+\xi}b}{\sqrt{\gamma}\sqrt{\gamma+\xi}}\left[2\sqrt{\gamma}\frac{\cosh\sqrt{\gamma}L - \cos\theta}{\sinh\sqrt{\gamma}L} + \lambda_0 + \sqrt{\gamma+\xi}\coth\sqrt{\gamma+\xi}b\right]. \tag{97}$$

The terms in the brackets correspond to the matrix[40] $\mathcal{M}$ (since $\lambda_1 = \infty$ we can consider only the element $\mathcal{M}_{00}$). The first term is the contribution of the loop, the second comes from the boundary condition and the last one comes from the arm. It immediately follows that

$$\int_0^\infty \mathrm{d}t\, \mathcal{F}_n(0, 0; t, \xi)\, \mathrm{e}^{-\gamma t} = \frac{1}{2\sqrt{\gamma}}\frac{\sinh\sqrt{\gamma}L}{\sinh\sqrt{\gamma}L_{\rm eff}}\, \mathrm{e}^{-|n|\sqrt{\gamma}L_{\rm eff}} \tag{98}$$

with

$$\cosh\sqrt{\gamma}L_{\rm eff} = \cosh\sqrt{\gamma}L + \tfrac{1}{2}\sqrt{1+\xi/\gamma}\sinh\sqrt{\gamma}L\coth\sqrt{\gamma+\xi}b. \tag{99}$$

Let us consider an infinitely long arm $b \to \infty$. If we are interested on time scales $t \gg \tau_L$, where $\tau_L = L^2$ is the Thouless time over which the ring is explored, equation (99) gives $\sqrt{\gamma}L_{\rm eff} \simeq (\gamma+\xi)^{1/4}\sqrt{L}$, therefore from equation (98) we see that $\mathcal{F}_n(0, 0; t, \xi) \simeq \mathrm{e}^{-\xi t}\mathcal{F}_n(0, 0; t, 0)$. The inverse Laplace transform of equation (95) leads to $\langle\delta(T - T_{\rm arm}[x])\rangle_{\mathcal{C}_n} \simeq \delta(T - t)$, which means that the Brownian motion spends almost all the time in the arm (this simple result confirms the picture presented to explain the scaling of the winding around the ring of the form $n_t \propto t^{1/4}$).

[40] The introduction of the conjugate parameters $\{\xi_{\alpha\beta}\}$ corresponds to shift the spectral parameter γ on each wire as $\gamma \to \gamma + \xi_{\alpha\beta}$. The matrix to be generalized is not M, given by equation (59), but $\mathcal{M} = \sqrt{\gamma}M$.

6. Planar Brownian motion and charged particle in a random magnetic field

A model of random magnetic field describing a charged particle moving in a plane and subjected to the random magnetic field $\mathcal{B}(\vec{r}) = \vec{\nabla} \times \vec{A}(\vec{r})$ due to an ensemble of magnetic Aharonov–Bohm vortices is described by the following Hamiltonian [77, 100]:

$$H = \frac{1}{2}(\vec{p} - \vec{A}(\vec{r}))^2 + \frac{1}{2}\mathcal{B}(\vec{r}) = \frac{1}{2}\left(\vec{p} - \alpha \sum_i \frac{\vec{u}_z \times (\vec{r} - \vec{r}_i)}{(\vec{r} - \vec{r}_i)^2}\right)^2 + \pi\alpha \sum_i \delta(\vec{r} - \vec{r}_i) \tag{100}$$

where $0 \leqslant \alpha < 1$. We have set $\hbar = e = m = 1$. α is the magnetic flux per vortex, in unit of the quantum flux $\phi_0 = h/e$: $\alpha = \phi/\phi_0 = \phi/(2\pi)$. The model is periodic in α with a period 1. $\vec{u}_z$ is the unit vector perpendicular to the plane. $\vec{r}_i$ are the positions of the vortices in the plane: they are uncorrelated random variables (Poisson distribution). The δ interactions (coupling to the magnetic field) are necessary in order to define properly the model [33, 63, 131, 163, 175].

By comparison with scalar impurities discussed in the introduction, the magnetic nature of the scatterers gives rise to rather different properties[41]: it was shown in [77] that the spectrum is reminiscent of a Landau spectrum with Landau levels broadened by disorder, in the limit of vanishing magnetic flux $\alpha \to 0$ (see below). This analysis was performed using perturbative arguments supported by numerical simulations. The latter use a relation between the average DoS of this particular model and some winding properties of the Brownian motion.

Let $Z(t)$ denotes the partition function for a given distribution of vortices and $Z_0(t)$ the partition function without fluxes. The ratio of partition functions can be written as a ratio of two path integrals

$$\frac{Z(t)}{Z_0(t)} = \frac{\int \mathrm{d}\vec{a} \int_{\vec{r}(0)=\vec{a}}^{\vec{r}(t)=\vec{a}} \mathcal{D}\vec{r}(\tau)\, \mathrm{e}^{\int_0^t (-\frac{1}{2}\dot{\vec{r}}^2 + \mathrm{i}\vec{A}\cdot\dot{\vec{r}})\mathrm{d}\tau}}{\int \mathrm{d}\vec{a} \int_{\vec{r}(0)=\vec{a}}^{\vec{r}(t)=\vec{a}} \mathcal{D}\vec{r}(\tau)\, \mathrm{e}^{-\int_0^t \frac{1}{2}\dot{\vec{r}}^2 \mathrm{d}\tau}} = \langle \mathrm{e}^{\mathrm{i}\oint_{\mathcal{C}} \vec{A}\cdot\mathrm{d}\vec{r}} \rangle_{\mathcal{C}}, \tag{101}$$

where $Z_0(t) = V/(2\pi t)$ is the free partition function (V is the (infinite) area of the plane) and $\langle \cdots \rangle_{\mathcal{C}}$ stands for averaging over all closed Brownian curves of the plane.

In order to average $Z(t)$ over the Poissonian distribution of vortices, let us consider, for a while, our problem on a square lattice with lattice spacing a. Let N_i be the number of vortices in square i. The magnetic flux through any closed random walk $\mathcal{C}$ on this lattice can be written as

$$\oint_{\mathcal{C}} \vec{A} \cdot \mathrm{d}\vec{r} = \sum_i 2\pi\alpha N_i n_i \tag{102}$$

where n_i is the number of times the square i has been wound around by $\mathcal{C}$.

Averaging $Z(t)$ with the Poisson distribution (μ being the mean density of vortices)

$$P(N_i) = \frac{(\mu a^2)^{N_i}}{N_i!}\, \mathrm{e}^{-\mu a^2} \tag{103}$$

gives

$$\langle Z(t) \rangle_{\{\vec{r}_i\}} = Z_0(t) \langle \mathrm{e}^{\mathrm{i}\oint_{\mathcal{C}} \vec{A}\cdot\mathrm{d}\vec{r}} \rangle_{\mathcal{C},\{\vec{r}_i\}} = Z_0(t) \left\langle \exp\left(\mu \sum_n S_n (\mathrm{e}^{2\mathrm{i}\pi\alpha n} - 1)\right) \right\rangle_{\mathcal{C}} \tag{104}$$

where $\langle \cdots \rangle_{\{\vec{r}_i\}}$ denotes averaging over the positions $\{\vec{r}_i\}$ of the vortices.

[41] For scalar impurities, the presence of a magnetic field also strongly affects the spectral properties. The case of a Gaussian disorder projected in the lowest Landau level (LLL) of a strong magnetic field was studied in [220]. Other disordered potentials were considered later. In particular it was shown in [46] that for a weak density of impurities, the spectrum can display power law singularities. A physical interpretation of such power law singularities has been discussed by Furtlehner in [100, 101]. The relation between the model of scalar impurities projected in the LLL of a strong magnetic field and the model of magnetic vortices was discussed in [78, 100]. Finally we mention a recent work on Lifshitz tails in the presence of a magnetic field [153].

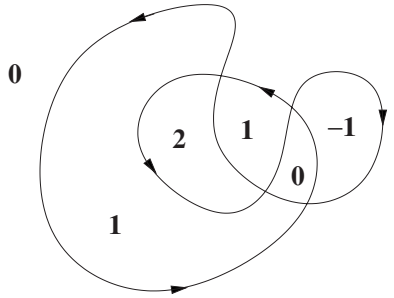

Figure 9. A closed curve with its n-winding sectors. The label n of a sector is the winding number of any point inside this sector.

The quantity S_n denotes the area of the locus of points around which the curve $\mathcal{C}$ has wound n times. This result was derived for a random walk on a lattice but is also obviously valid off lattice as well, for Brownian curves. The winding sectors of a closed curve are displayed in figure 9.

The random variable S_n scales like t. In particular, we know [62, 118] its expectation $\langle S_n \rangle = \frac{t}{2\pi n^2}$. Moreover, it has been shown in [223] that the variable $n^2 S_n$ becomes more and more peaked when n grows: $P(n^2 S_n = X) \underset{n\to\infty}{\longrightarrow} \delta\big(X - \frac{t}{2\pi}\big)$ (the average area of the $n = 0$-sector has recently been studied in [104]).

Thus, extracting t, equation (104) is rewritten as

$$\langle Z(t)\rangle_{\{\vec{r}_i\}} = Z_0(t) \int \mathrm{d}S\, \mathrm{d}A\; P(S, A)\, \mathrm{e}^{-\mu t(S+\mathrm{i}A)} \equiv Z_0(t) \langle \mathrm{e}^{-\mu t(S+\mathrm{i}A)} \rangle_{\mathcal{C}}, \tag{105}$$

where $P(S, A)$ is the joint distribution of the rescaled (t independent) variables S and A defined as

$$S = \frac{2}{t} \sum_n S_n \sin^2(\pi\alpha n) \tag{106}$$

$$A = \frac{1}{t} \sum_n S_n \sin(2\pi\alpha n). \tag{107}$$

The averages of these two variables are given by

$$\langle S \rangle = \pi\alpha(1 - \alpha) \tag{108}$$

$$\langle A \rangle = 0. \tag{109}$$

With equation (105), we observe that $\frac{1}{V}\langle Z(t)\rangle_{\{\vec{r}_i\}}$ has the scaling form $F(\mu t)/t$. Thus, its inverse Laplace transform, the average density of states per unit area, is a function of only E/μ and α. Moreover, it is easy to realize that $\langle Z(t)\rangle_{\{\vec{r}_i\}}$ is even in α (each Brownian curve in $\{\mathcal{C}\}$ comes with its time reversed) and periodic in α with period 1. Thus, one can restrict to $0 \leqslant \alpha \leqslant \frac{1}{2}$. Let us focus on the two limiting cases $\alpha \to 0$ and $\alpha = 1/2$.

- *Limit $\alpha \to 0$: Landau spectrum.*
  When $\alpha \to 0$, a careful analysis shows that

  $$\langle Z(t)\rangle_{\{\vec{r}_i\}} \simeq Z_{\langle\mathcal{B}\rangle}\, \mathrm{e}^{-\frac{1}{2}\langle\mathcal{B}\rangle t} \tag{110}$$

  where $Z_{\langle\mathcal{B}\rangle} = Z_0(t) \frac{\langle\mathcal{B}\rangle t/2}{\sinh(\langle\mathcal{B}\rangle t/2)}$ is the partition function of a charged particle in a uniform magnetic field $\langle\mathcal{B}\rangle = 2\pi\mu\alpha$ (we recall that the impurity i carries a magnetic field

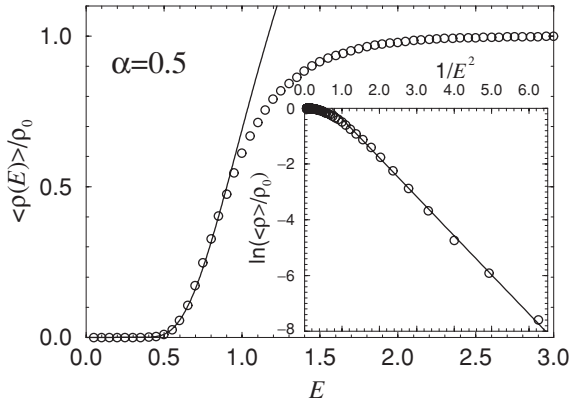

Figure 10. The average density of states at $\alpha = 0.5$ (the free density of states is constant $\rho_0 = 1/(2\pi)$). Circles are simulation results. The full line is the fit discussed in the text.

$2\pi\alpha\delta(\vec{r} - \vec{r}_i)$). The system of random vortices is, thus, equivalent to the uniform average magnetic field, albeit with an additional positive shift in the Landau spectrum: the inverse Laplace transform of the partition function (110) gives the Landau spectrum made of equally spaced infinitely degenerated levels. This corresponds to the oscillating behaviour shown in figure 11. The origin of the shift can be traced back to the presence of the repulsive δ interactions that have been added to the Hamiltonian to define properly the model.

- *Half quantum flux vortices* ($\alpha = 1/2$)—*the spectral singularity at* $E = 0$.
In this case variable (107) vanishes, $A \equiv 0$, implying that $\langle Z(t)\rangle_{\{\vec{r}_i\}} = Z_0(t)\langle\exp(-\mu t S)\rangle_C$ where now

$$S = \frac{2}{t}\sum_{n\ \text{odd}} S_n. \tag{111}$$

Performing the inverse Laplace transform, we get the average density of states per unit area:

$$\langle\rho(E)\rangle = \rho_0(E)\int_0^{E/\mu} \mathrm{d}S\,P(S) \tag{112}$$

where $\rho_0(E) = \frac{1}{2\pi}$ is the free density of states per unit area and $P(S)$ is the probability distribution of S.

We may use this result to determine the nature of the singularity in the average DoS. As displayed in figure 10 (where we have taken $\mu = 1$), $\langle\rho(E)\rangle$ increases monotonically from 0 to $\rho_0(E)$ with a depletion of states at the bottom of the spectrum. Circles are the result of numerical simulations (on a 2D square lattice, we have generated 10 000 closed random walks of 100 000 steps each). The full line is a low-energy fit of the quantity $\langle\rho(E)\rangle/\rho_0$ by the function

$$\frac{\rho_{\text{fit}}(E)}{\rho_0} = a\,\mathrm{e}^{-b(\mu/E)^2} \tag{113}$$

with $a = 2.8$ and $b = 1.4$ (see figure 10). It is worth stressing that this behaviour is quite different from that expected for a disorder due to a scalar potential. The famous Lifshitz

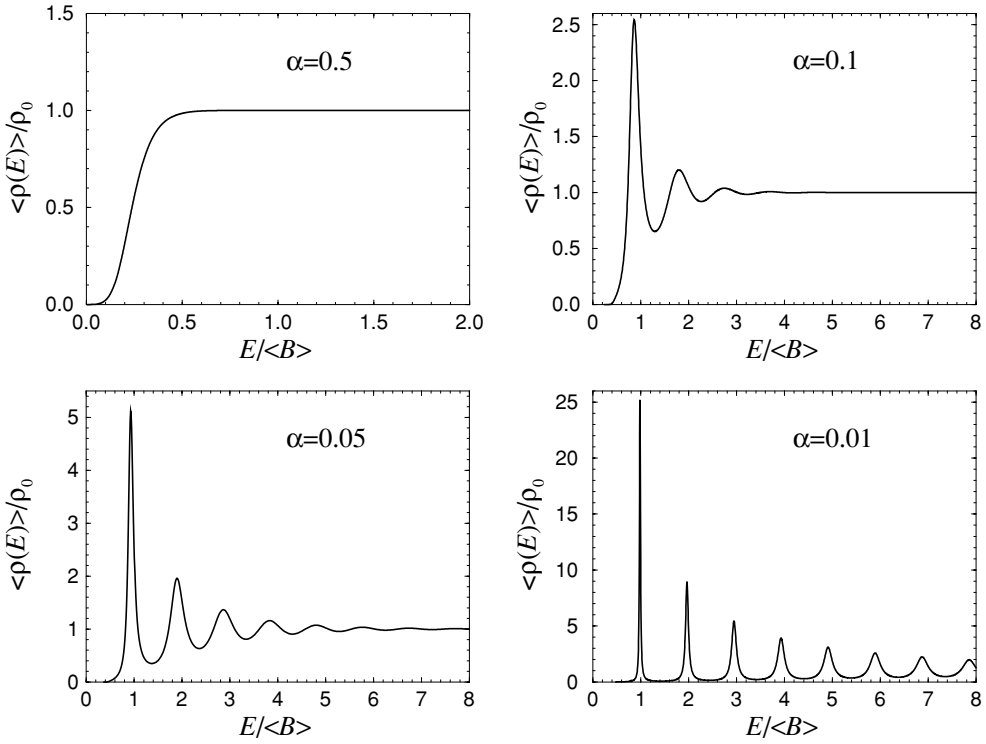

Figure 11. Average density of states of the Hamiltonian (100) for different values of the flux per tube $\phi = \alpha\phi_0$. The average magnetic field reads $\langle\mathcal{B}\rangle = 2\pi\mu\alpha$. We recall that the corresponding Landau spectrum is given by $E_n = \langle\mathcal{B}\rangle(n+1)$, for $n \geqslant 0$ (from [77]).

argument, applicable to the low-energy DoS for a low concentration of *scalar* impurity, leads instead to[42] a behaviour

$$\rho_{\mathrm{Lif}}(E) \sim \mathrm{e}^{-c_2\mu/E}, \tag{114}$$

where c_2 is a constant. Our choice for this fit is motivated by a recent numerical work [184] concerning the area $\mathcal{A}$ of the outer boundary of planar random loops. In this work, the author suggests that the limit distribution of $\mathcal{A}$ is the Airy distribution implying, for small $\mathcal{A}$ values, a behaviour of the type $\exp(-\mathrm{const}/\mathcal{A}^2)/\mathcal{A}^2$. Remarking that $\mathcal{A} = \sum_{n\,\mathrm{even}} S_n + \sum_{n\,\mathrm{odd}} S_n$, it is natural to expect for the distribution of the random variable S, equation (111), a behaviour at small S that is roughly given by $\exp(-\mathrm{const}/S^2)$. Thus, we deduce the form $\rho_{\mathrm{fit}}(E)$ for the low-energy fit of $\langle\rho(E)\rangle$.

- *Transition between* $\alpha = 0.5$ *and* $\alpha \to 0$.

  Finally, when α grows from 0 to 0.5, the oscillations in the spectrum must disappear at some critical value α_c (see figure 11). Numerical simulations, specific heat considerations and, also, diagrammatic expansions [77] give $\alpha_c \sim 0.3$.

[42] The Lifshitz argument applies to the DoS for the random Hamiltonian $H = -\Delta + \sum_i u(\vec{r} - \vec{r}_i)$ in dimension d, where $u(\vec{r})$ is a sharply peaked scalar potential. For a low density of impurities μ, the DoS behaves as $\rho_{\mathrm{Lif}}(E) \sim \exp(-c_d\mu/E^{d/2})$ at low energy.

7. Conclusion

A non-experienced reader may have the feeling that the two topics which have been covered in this review, namely one-dimensional disordered systems and quantum graphs, are essentially disjoint. In fact there are many interesting links between these two topics, both at a methodological and a conceptual level. The use of metric graphs for modelling quantum phenomena observed in disordered metals goes back to the pioneering work of Shapiro [191] and Chalker and Coddington [56]. These systems have been used to study quantum localization and more recently as a model system for spectral statistics (for a recent review, see [202]). Another set of similar questions is provided by the study of scattering properties of chaotic graphs [143] and disordered systems [103] (see also section 3.2 and [174] for recent developments). We have also seen that apart from its interest to study the spectral properties of metric graphs, the spectral determinant also allows studying several properties of networks of quasi-one-dimensional weakly disordered wires [3, 177, 178].

As a conclusion we would like to mention several open problems.

- A study of spectral statistics in the case of graphs with a random Schrödinger operator (there is still a factorized structure but the matrix R is now given by equation (66)).
- A probabilistic understanding of the star graphs using the tools of excursion theory developed by Barlow *et al* [23] in the context of the Brownian spider. A first step would be to recover those probabilistic results (the joint law of the occupation time inside the branches) by a spectral approach. It is however not excluded that the probabilistic approach could provide a key to a deeper understanding of those quantum systems. In the context of classical systems such probabilistic approaches have been very useful, e.g. recent studies of the stochastic Loewner equation have made enormous progress in understanding the statistical physics of a class of two-dimensional systems. This calls for new probabilistic techniques for quantum systems as well.
- Several functionals of Brownian motion (13), (16) appear when studying the important question of dephasing due to electron–electron interaction in networks of quasi-one-dimensional weakly disordered wires. The fact that such simple functionals appear relies on the translation invariance of the two particular problems studied (an infinite wire [9] and an isolated ring [212]). For a network with arbitrary topology, the relevant functional of the Brownian bridge $x(\tau)$ is given by $\int_0^t \mathrm{d}\tau\, W(x(\tau), x(t-\tau))$ where $W(x,x') = \frac{1}{2}[P_d(x,x) + P_d(x',x')] - P_d(x,x')$ with $-\Delta P_d(x,x') = \delta(x-x')$. It now involves a nonlocal functional in time which is difficult to handle. Progress in this direction would allow clarification of the interplay between the electron–electron interaction and the geometrical effect and help in analysing recent experimental results [29, 94].
- The question of extreme value spectral statistics was addressed in the framework of random matrix theory [214] and these studies have found several applications in the context of out-of-equilibrium statistical physics (see the review [215]). However this question was first addressed in the context of one-dimensional disordered systems [117]. The study of supersymmetric random Hamiltonian, for which the bottom of the spectrum plays a special role, has emphasized the interest in extreme value spectral statistics [204] (in particular it indicates level correlations). It would be interesting to extend such studies to other models and find some physical situations where these results would be applicable.
- A beautiful heuristic argument was provided by Lifshitz to explain the spectral singularity for Hamiltonians with a weak concentration of localized scalar impurities (see for example the book [157]). Other mechanisms should be invoked to explain the nature of the quantum states responsible for the low-energy power law behaviour in the case of a uniform strong

magnetic field with δ-impurities [100, 101]. For the model of randomly distributed magnetic fluxes, the numerical simulations for $\alpha = 1/2$ have suggested the new type of singular behaviour (113). It would be interesting to provide heuristic arguments to understand more deeply the origin of this singularity.

Acknowledgments

The review gives an overview of several joint works involving Éric Akkermans, Cyril Furtlehner, Satya Majumdar, Gilles Montambaux, Cécile Monthus, Stéphane Ouvry and Marc Yor. We thank them for fruitful collaborations. Meanwhile we have also benefited from stimulating discussions with Marc Bocquet, Eugène Bogomolny, Oriol Bohigas, Hélène Bouchiat, Markus Büttiker, David Dean, Richard Deblock, Meydi Ferrier, Sophie Guéron, Jean-Marc Luck, Gleb Oshanin, Leonid Pastur and Denis Ullmo. We are pleased to acknowledge Satya Majumdar for his careful reading and valuable remarks.

References

[1] Abrahams E, Anderson P W, Licciardello D C and Ramakrishnan T V 1979 Scaling theory of localization: absence of quantum diffusion in two dimensions *Phys. Rev. Lett.* **42** 673
[2] Adamyan V 1992 Scattering matrices for microschemes *Oper. Theory: Adv. Appl.* **59** 1
[3] Akkermans E, Comtet A, Desbois J, Montambaux G and Texier C 2000 On the spectral determinant of quantum graphs *Ann. Phys., NY* **284** 10–51
[4] Akkermans É and Montambaux G 2004 Physique mésoscopique des électrons et des photons *EDP Sciences* CNRS édn (Paris: CNRS)
[5] Albeverio S, Gesztesy S A, Hoegh-Krohn R and Holden H 2004 *Solvable Models in Quantum Mechanics (AMS Chelsea Publishing)* 2nd edn (New York: Chelsea)
[6] Alexander S 1983 Superconductivity of networks: a percolation approach to the effects of disorder *Phys. Rev.* B **27** 1541
[7] Altland A and Zirnbauer M R 1997 Nonstandard symmetry classes in mesoscopic normal-superconducting hybrid structures *Phys. Rev.* B **55** 1142
[8] Al'tshuler B L and Aronov A G 1981 Magnetoresistance of thin films and of wires in a longitudinal magnetic field *JETP Lett.* **33** 499
[9] Altshuler B L, Aronov A G and Khmelnitsky D E 1982 Effects of electron–electron collisions with small energy transfers on quantum localisation *J. Phys. C: Solid State. Phys.* **15** 7367
[10] Al'tshuler B L, Aronov A G and Spivak B Z 1981 The Aharonov–Bohm effect in disordered conductors *JETP Lett.* **33** 94
[11] Al'tshuler B L, Aronov A G, Spivak B Z, Sharvin D Yu and Sharvin Yu V 1982 Observation of the Aharonov–Bohm effect in hollow metal cylinders *JETP Lett.* **35** 588
[12] Al'tshuler B L, Khmel'nitzkiĭ D E, Larkin A I and Lee P A 1980 Magnetoresistance and Hall effect in a disordered two-dimensional electron gas *Phys. Rev.* B **22** 5142
[13] Al'tshuler B L and Lee P A 1988 Disordered electronic systems *Phys. Today* **41** 36
[14] Altshuler B L and Prigodin V N 1989 Distribution of local density of states and NMR line shape in a one-dimensional disordered conductor *Sov. Phys.—JETP* **68** 198
[15] Antsygina T N, Pastur L A and Slyusarev V A 1981 Localization of states and kinetic properties of one-dimensional disordered systems *Sov. J. Low Temp. Phys.* **7** 1–21
[16] Aronov A G and Sharvin Yu V 1987 Magnetic flux effects in disordered conductors *Rev. Mod. Phys.* **59** 755
[17] Ashcroft N W and Mermin N D 1976 *Solid State Physics* (Philadelphia, PA: Saunders)
[18] Avron J E, Exner P and Last Y 1994 Periodic Schrödinger operators with large gaps and Wannier–Stark ladders *Phys. Rev. Lett.* **72** 896
[19] Avron J E, Raveh A and Zur B 1988 Adiabatic quantum transport in multiply connected systems *Rev. Mod. Phys.* **60** 873
[20] Avron J E and Sadun L 1991 Adiabatic quantum transport in networks with macroscopic components *Ann. Phys., NY* **206** 440
[21] Azbel M Ya 1983 Resonance tunneling and localization spectroscopy *Solid State Commun.* **45** 527
[22] Ball R C, Havlin S and Weiss G H 1987 Non-Gaussian random walks *J. Phys. A: Math. Gen.* **20** 4055

[23] Barlow M, Pitman J and Yor M 1989 *Une Extension Multidimensionnelle de la loi de L'arc Sinus (Lecture Notes in Maths* vol 1372*)* (Berlin: Springer) p 294
[24] Barra F and Gaspard P 2000 On the level spacing distribution in quantum graphs *J. Stat. Phys.* **101** 283
[25] Barra F and Gaspard P 2001 Transport and dynamics on open quantum graphs *Phys. Rev.* E **65** 016205
[26] Bartholdi L 1999 Counting paths in graphs *L'Enseignement Math.* **45** 83
[27] Barzykin A V and Tachiya M 1993 Diffusion-influenced reaction kinetics on fractal structures *J. Chem. Phys.* **99** 9591
[28] Bass H 1992 The Ihara–Selberg zeta function of a tree lattice *Int. J. Math.* **3** 717
[29] Bauërle C, Mallet F, Montambaux G, Saminadayar L, Schopfer F and Texier C 2005 in preparation
[30] Beenakker C W J 1997 Random-matrix theory of quantum transport *Rev. Mod. Phys.* **69** 731–808
[31] Bending S J, Klitzing K von and Ploog K 1990 Weak localization in a distribution of magnetic flux tubes *Phys. Rev. Lett.* **65** 1060
[32] Berezinskiĭ V L 1974 Kinetics of a quantum particle in a one-dimensional random potential *Sov. Phys.—JETP* **38** 620
[33] Bergman O and Lozano G 1994 Aharonov–Bohm scattering, contact interactions and scale invariance *Ann. Phys., NY* **229** 416
[34] Bergmann G 1984 Weak localization in thin films *Phys. Rep.* **107** 1
[35] Berkolaiko G, Bogomolny E B and Keating J P 2001 Star graphs and Šeba billiards *J. Phys. A: Math. Gen.* **34** 335
[36] Berkolaiko G and Keating J P 1999 Two-point spectral correlations for star graphs *J. Phys. A: Math. Gen.* **32** 7827
[37] Beth E and Uhlenbeck G E 1937 *Physica* **4** 915
[38] Bocquet M 1999 Some spectral properties of the one-dimensional disordered Dirac equation *Nucl. Phys.* B [FS] **546** 621
[39] Bocquet M 2000 Chaînes de spins, fermions de Dirac et systèmes désordonnés *PhD Thesis* École Polytechnique, available at http://tel.ccsd.cnrs.fr/documents/archives0/00/00/15/60/
[40] Bocquet M, Serban D and Zirnbauer M R 2000 Disordered 2d quasiparticles in class D: Dirac fermions with random mass, and dirty superconductors *Nucl. Phys.* B [FS] **578** 628
[41] Bouchaud J-P, Comtet A, Georges A and Le Doussal P 1987 The relaxation-time spectrum of diffusion in a one-dimensional random medium: an exactly solvable case *Europhys. Lett.* **3** 653
[42] Bouchaud J-P, Comtet A, Georges A and Le Doussal P 1990 Classical diffusion of a particle in a one-dimensional random force field *Ann. Phys., NY* **201** 285–341
[43] Bouchaud J-P and Georges A 1990 Anomalous diffusion in disordered media: statistical mechanisms, models and physical applications *Phys. Rep.* **195** 267
[44] Bouchaud J-P and Mézard M 1997 Universality classes for extreme value statistic *J. Phys. A: Math. Gen.* **30** 7997
[45] Bougerol P and Lacroix J 1985 *Products of Random Matrices with Applications to Schrödinger Operators* (Basle: Birkhäuser)
[46] Brézin É, Gross D J and Itzykson C 1984 Density of states in the presence of a strong magnetic field and random impurities *Nucl. Phys.* B [FS] **235** 24
[47] Brouwer P W, Frahm K M and Beenakker C W 1997 Quantum mechanical time-delay matrix in chaotic scattering *Phys. Rev. Lett.* **78** 4737
[48] Brouwer P W, Mudry C and Furusaki A 2000 Density of states in coupled chains with off-diagonal disorder *Phys. Rev. Lett.* **84** 2913
[49] Brouwer P W, Mudry C and Furusaki A 2003 Universality of delocalization in unconventional dirty superconducting wires with broken spin-rotation symmetry *Phys. Rev.* B **67** 014530
[50] Büttiker M 1990 Traversal, reflection and dwell time for quantum tunneling *Electronic Properties of Multilayers and Low-Dimensional Semiconductors Structures* ed J M Chamberlain *et al* (New York: Plenum) p 297
[51] Büttiker M 2002 Charge densities and charge noise in mesoscopic conductors *Pramana J. Phys.* **58** 241 (*Preprint* cond-mat/0112330)
[52] Büttiker M, Imry Y and Azbel M Ya 1984 Quantum oscillations in one-dimensional normal-metal rings *Phys. Rev.* A **30** 1982
[53] Carlier F and Akulin V M 2004 Quantum interference in nanofractals and its optical manifestation *Phys. Rev.* B **69** 115433
[54] Carpentier D and Le Doussal P 2001 Glass transition of a particle in a random potential, front selection and entropic phenomena in Liouville and sinh-Gordon models *Phys. Rev.* E **63** 026110
[55] Chakravarty S and Schmid A 1986 Weak localization: the quasiclassical theory of electrons in a random potential *Phys. Rep.* **140** 193

[56] Chalker J T and Coddington P D 1988 Percolation, quantum tunnelling and the integer Hall-effect *J. Phys. C: Solid State Phys.* **21** 2665

[57] Chekhov L O 1999 A spectral problem on graphs and L-functions *Russ. Math. Surv.* **54** 1197

[58] Cifarelli D M and Regazzini E 1975 Contributi intorno ad un test per l'homogeneita tra du campioni *G. Econ.* **34** 233–49

[59] Colin de Verdière Y 1998 *Spectres de Graphes* (Société Mathématique de France)

[60] Comtet A, Desbois J and Majumdar S N 2002 The local time distribution of a particle diffusing on a graph *J. Phys. A: Math. Gen.* **35** L687

[61] Comtet A, Desbois J and Monthus C 1995 Localization properties in one-dimensional disordered supersymmetric quantum mechanics *Ann. Phys., NY* **239** 312–50

[62] Comtet A, Desbois J and Ouvry S 1990 Winding of planar Brownian curves *J. Phys. A: Math. Gen.* **23** 3563

[63] Comtet A, Mashkevich S and Ouvry S 1995 Magnetic moment and perturbation theory with singular magnetic fields *Phys. Rev.* D **52** 2594

[64] Comtet A, Monthus C and Yor M 1998 Exponential functionals of Brownian motion and disordered systems *J. Appl. Probab.* **35** 255

[65] Comtet A and Texier C 1997 On the distribution of the Wigner time delay in one-dimensional disordered systems *J. Phys. A: Math. Gen.* **30** 8017–25

[66] Comtet A and Texier C 1998 One-dimensional disordered supersymmetric quantum mechanics: a brief survey *Supersymmetry and Integrable Models: Proc. Workshop (Chicago, IL, June 1997) (Lecture Notes in Physics* vol 502*)* ed H Aratyn, T D Imbo, W-Y Keung and U Sukhatme (Berlin: Springer) pp 313–28 (also available at *Preprint* cond-mat/9707313)

[67] Dashen R, Ma S-K and Bernstein H J 1969 S-matrix formulation of statistical mechanics *Phys. Rev.* **187** 345

[68] de Calan C, Luck J-M, Nieuwenhuizen T M and Pétritis D 1985 On the distribution of a random variable occurring in 1D disordered systems *J. Phys. A: Math. Gen.* **18** 501

[69] de Carvalho C A A and Nussenzveig H M 2002 Time delay *Phys. Rep.* **364** 83

[70] Dean D S and Majumdar S N 2001 Extreme value statistics of hierarchically correlated variables: deviation from Gumbel statistics and anomalous persistence *Phys. Rev.* E **64** 046121

[71] Derrida B 1983 Singular behaviour of certain infinite products of random 2×2 matrices *J. Phys. A: Math. Gen.* **16** 2641

[72] Desbois J 2000 Spectral determinant of Schrödinger operators on graphs *J. Phys. A: Math. Gen.* **33** L63

[73] Desbois J 2000 Time-dependent harmonic oscillator and spectral determinant on graphs *Eur. Phys. J.* B **15** 201

[74] Desbois J 2001 Spectral determinant on graphs with generalized boundary conditions *Eur. Phys. J.* B **24** 261

[75] Desbois J 2002 Occupation times distribution for Brownian motion on graphs *J. Phys. A: Math. Gen.* **35** L673

[76] Desbois J and Comtet A 1992 Algebraic areas enclosed by Brownian curves on bounded domains *J. Phys. A: Math. Gen.* **25** 3095

[77] Desbois J, Furtlehner C and Ouvry S 1995 Random magnetic impurities and the Landau problem *Nucl. Phys.* B [FS] **453** 759–76

[78] Desbois J, Furtlehner C and Ouvry S 1996 Random magnetic impurities and the δ impurity problem *J. Phys.* I *(France)* **6** 641–8

[79] Dorokhov O N 1982 Transmission coefficient and the localization length of an electron in N bound disordered chains *JETP Lett.* **36** 318

[80] Dorokhov O N 1988 Solvable model of multichannel localization *Phys. Rev.* B **37** 10526

[81] Douçot B and Rammal R 1985 Quantum oscillations in normal-metal networks *Phys. Rev. Lett.* **55** 1148

[82] Douçot B and Rammal R 1986 Interference effects and magnetoresistance oscillations in normal-metal networks: 1. weak localization approach *J. Physique* **47** 973–99

[83] Dyson F J 1953 The dynamics of a disordered linear chain *Phys. Rev.* **92** 1331

[84] Echternach P M, Gershenson M E, Bozler H M, Bogdanov A L and Nilsson B 1993 Nyquist phase relaxation in one-dimensional metal films *Phys. Rev.* B **48** 11516

[85] Edwards S F 1967 Statistical mechanics with topological constraints *Proc. Phys. Soc.* **91** 513

[86] Efetov K 1997 *Supersymmetry in Disorder and Chaos* (Cambridge: Cambridge University Press)

[87] Efros A L and Pollak M (ed) 1985 *Electron–Electron Interactions in Disordered Systems* (Amsterdam: North-Holland)

[88] Evangelou S N and Katsanos D E 2003 Spectral statistics in chiral-orthogonal disordered systems *J. Phys. A: Math. Gen.* **36** 3237

[89] Exner P 1995 Lattice Kronig-Penney models *Phys. Rev. Lett.* **74** 3503

[90] Exner P 1996 Contact interactions on graph superlattices *J. Phys. A: Math. Gen.* **29** 87

[91] Fabrizio M and Mélin R 1997 Coexistence of antiferromagnetism and dimerization in a disordered spin-Peierls model: exact results *Phys. Rev. Lett.* **78** 3382

[92] Fabrizio M and Mélin R 1997 Enhanced magnetic fluctuations in doped spin-Peierls systems: a single-chain-model analysis *Phys. Rev.* B **56** 5996

[93] Faris W G and Tsay W J 1994 Time delay in random scattering *SIAM J. Appl. Math.* **54** 443

[94] Ferrier M, Angers L, Rowe A C H, Guéron S, Bouchiat H, Texier C, Montambaux G and Mailly D 2004 Direct measurement of the phase coherence length in axs GaAs/GaAlAs square network *Phys. Rev. Lett.* **93** 246804

[95] Flajeolet P and Louchard G 2001 Analytic variations on the Airy distribution *Algorithmica* **31** 361

[96] Forman R 1987 Functional determinants and geometry *Invent. Math.* **88** 447

[97] Friedel J 1952 The distribution of electrons round impurities in monovalent metals *Phil. Mag.* **43** 153

[98] Friedel J 1958 Metallic alloys *Nuovo Cimento Suppl.* **7** 287

[99] Frisch H L and Lloyd S P 1960 Electron levels in a one-dimensional random lattice *Phys. Rev.* **120** 1175

[100] Furtlehner C 1997 Étude du spectre de Landau pour un champ magnétique aléatoire en dimension 2 *PhD Thesis* Université Paris 6

[101] Furtlehner C 2000 Lifshitz-like argument for low-lying states in a strong magnetic field *Eur. Phys. J.* B **18** 297

[102] Fyodorov Y V and Sommers H-J 1996 Parametric correlations of scattering phase shifts and fluctuations of delay times in few-channel chaotic scattering *Phys. Rev. Lett.* **76** 4709

[103] Fyodorov Y V and Sommers H-J 1997 Statistics of resonance poles, phase shift and time delays in quantum chaotic scattering: random matrix approach for systems with broken time-reversal invariance *J. Math. Phys.* **38** 1918

[104] Garban C and Trujillo Ferreras J A 2005 The expected area of the filled planar Brownian loop is $\pi/5$, unpublished (*Preprint* math.PR/0504496)

[105] Gardiner C W 1989 *Handbook of Stochastic Methods for Physics, Chemistry and the Natural Sciences* (Berlin: Springer)

[106] Gefen Y, Imry Y and Azbel M Ya 1984 Quantum oscillations and the Aharonov–Bohm effect for parallel resistors *Phys. Rev. Lett.* **52** 129

[107] Geim A K 1989 Nonlocal magnetoresistance of bismuth films in nonuniform field of Abrikosov vortices *JETP Lett.* **50** 389

[108] Gerasimenko N I and Pavlov B S 1988 Scattering problems on noncompact graphs *Theor. Math. Phys.* **74** 230

[109] Gershenson M E, Khavin Yu B, Mikhalchuk A, Bolzer H M and Bogdanov A L 1997 Crossover from weak to strong localization in quasi-one-dimensional conductors *Phys. Rev. Lett.* **79** 725

[110] Gnutzmann S and Altland A 2004 Universal spectral statistics in quantum graphs *Phys. Rev. Lett.* **93** 194101

[111] Gogolin A A and Mel'nikov V I 1977 Conductivity of one-dimensional metal with half-filled band *Sov. Phys.—JETP* **46** 369

[112] Gogolin A A, Mel'nikov V I and Rashba E I 1976 Conductivity in a disordered one-dimensional system induced by electron–phonon interaction *Sov. Phys.—JETP* **42** 168

[113] Gol'dshtein I Ya, Molchanov S A and Pastur L A 1977 A pure point spectrum of the stochastic one-dimensional Schrödinger operator *Funct. Anal. Appl.* **11** 1

[114] Gopar V A, Mello P A and Büttiker M 1996 Mesoscopic capacitors: a statistical analysis *Phys. Rev. Lett.* **77** 3005

[115] Gor'kov L P, Dorokhov O N and Prigara F V 1983 Structure of wavefunctions an ac conductivity id disordered one-dimensional conductors *Sov. Phys.—JETP* **58** 852

[116] Gor'kov L P, Larkin A I and Khmel'nitzkiĭ D E 1979 Particle conductivity in a two-dimensional random potential *JETP Lett.* **30** 228

[117] Grenkova L N, Molčanov S A and Sudarev J N 1983 On the basic states of one-dimensional disordered structures *Commun. Math. Phys.* **90** 101

[118] Grosberg A and Frisch H 2003 Winding angle distribution for planar random walk, polymer ring entangled with an obstacle, and all that: Spitzer–Edwards–Prager–Frisch model revisited *J. Phys. A: Math. Gen.* **36** 895

[119] Gumbel E J 1935 Les valeurs extrê mes des distributions statistiques *Ann. Inst. H Poincaré* **5** 115

[120] Gumbel E J 1954 *Statistical Theory of Extreme Values and Some Practical Applications (National Bureau of Standards Applied Mathematics Series* 33*)* Issued February 12

[121] Gumbel E J 1958 *Statistics of Extremes* (New York: Columbia University Press)

[122] Gurarie V and Chalker J T 2003 Bosonic excitations in random media *Phys. Rev.* B **68** 134207

[123] Gutzwiller M G 1990 *Chaos in Classical and Quantum Mechanics Interdisciplinary Applied Mathematics* vol 1 (New York: Springer)

[124] Halperin B I 1965 Green's functions for a particle in a one-dimensional random potential *Phys. Rev.* **139** A104

[125] Hauge E H and Støvneng J A 1989 Tunneling times: a critical review *Rev. Mod. Phys.* **61** 917

[126] Heinzner P, Huckleberry A and Zirnbauer M R 2005 Symmetry classes of disordered fermions *Commun. Math. Phys.* **257** 725
[127] Hikami S, Larkin A I and Nagaoka Y 1980 Spin–orbit interaction and magnetoresistance in the two dimensional random system *Prog. Theor. Phys.* **63** 707
[128] Igloi F and Monthus C 2005 Strong disorder RG approach of random systems *Phys. Rep.* **412** 277
[129] Ihara Y 1966 On discrete subgroup of the two by two projective linear group over p-adic field *J. Math. Soc. Japan* **18** 219
[130] Itzykson C and Drouffe J-M 1989 *Théorie Statistique des Champs* tomes 1 and 2 (Paris: EDP Sciences, Interéditions–CNRS)
[131] Jackiw R and Pi S Y 1990 Classical and quantal nonrelativistic Chern–Simons theory *Phys. Rev.* D **42** 3500
[132] Jayannavar A M, Vijayagovindan G V and Kumar N 1989 Energy dispersive backscattering of electrons from surface resonances of a disordered medium and $1/f$ noise *Z. Phys. B: Condens. Matter* **75** 77
[133] Jeanblanc M, Pitman J and Yor M 1997 The Feynman–Kac formula and decomposition of Brownian paths *Comput. Appl. Math.* **16** 27
[134] Jona-Lasinio G 1983 Qualitative theory of stochastic differential equations and quantum mechanics of disordered systems *Helv. Phys. Act.* **56** 61
[135] Kac M 1946 On the average of a certain Wiener functional and a related limit theorem in calculus of probability *Trans. Am. Math. Soc.* **59** 401
[136] Keating J P, Marklof J and Winn B 2003 Value distribution of the eigenfunctions and spectral determinants of quantum star graphs *Commun. Math. Phys.* **241** 421
[137] Keldysh L V 1964 Deep levels in semiconductors *Sov. Phys.—JETP* **18** 253
[138] Kesten H 1973 *Acta Math.* **131** 208
[139] Kostrykin V and Schrader R 1999 Kirchhoff's rule for quantum wires *J. Phys. A: Math. Gen.* **32** 595
[140] Kottos T and Smilansky U 1997 Quantum chaos on graphs *Phys. Rev. Lett.* **79** 4794
[141] Kottos T and Smilansky U 1999 Periodic orbit theory and spectral statistics for quantum graphs *Ann. Phys., NY* **274** 76
[142] Kottos T and Smilansky U 2000 Chaotic scattering on graphs *Phys. Rev. Lett.* **85** 968
[143] Kottos T and Smilansky U 2003 Quantum graphs: a simple model for chaotic scattering *J. Phys. A: Math. Gen.* **36** 3501
[144] Krein M G 1953 Trace formulas in perturbation theory *Matem. Sbornik* **33** 597
[145] Kuchinskii E Z and Sadovskii M V 1998 Combinatorics of Feynman diagrams for the problems with Gaussian random field *Sov. Phys.—JETP* **86** 367
[146] Kuchment P 2004 Quantum graphs: I. Some basic structures *Waves Random Media* **14** S107
[147] Kuchment P 2005 Quantum graphs: II. Some spectral properties of quantum and combinatorial graphs *J. Phys. A: Math. Gen.* **38** 4887
[148] Landau L D and Lifchitz E 1966 *Physique Statistique* tome V (Paris: Mir)
[149] Landauer R and Martin T 1994 Barrier interaction time in tunneling *Rev. Mod. Phys.* **66** 217
[150] Le Doussal P, Monthus C and Fisher D S 1999 Random walkers in one-dimensional random environments: exact renormalization group analysis *Phys. Rev.* E **59** 4795
[151] Le Gall J-F 1992 *Some Properties of Planar Brownian Motion (Lectures Notes in Maths)* (Berlin: Springer) p 1527
[152] Lee P A and Ramakrishnan T V 1985 Disordered electronic systems *Rev. Mod. Phys.* **57** 287
[153] Leschke H and Warzel S 2004 Quantum-classical transitions in Lifshitz tails with magnetic fields *Phys. Rev. Lett.* **92** 086402
[154] Leuridan C 2000 Théorème de Ray–Knight dans un arbre: une approche algébrique, Prépublication de l'ínstitut Fourier no 509 http://www-fourier.ujf-grenoble.fr/prepublications.html
[155] Lévy P 1948 *Processus Stochastiques et Mouvement Brownien (Éditions Jacques Gabay)* (Paris: Jacques Gabay)
[156] Licciardello D C and Thouless D J 1975 Constancy of minimum metallic conductivity in two dimensions *Phys. Rev. Lett.* **35** 1475
[157] Lifshits I M, Gredeskul S A and Pastur L A 1988 *Introduction to the Theory of Disordered Systems* (New York: Wiley)
[158] Luck J-M 1992 *Systèmes Désordonnés Unidimensionnels* (Aléa Saclay)
[159] Ludwig T and Mirlin A D 2004 Interaction-induced dephasing of Aharonov–Bohm oscillations *Phys. Rev.* B **69** 193306
[160] Majumdar S N and Comtet A 2004 Exact maximal height distribution of fluctuating interfaces *Phys. Rev. Lett.* **92** 225501

[161] Majumdar S N and Comtet A 2005 Airy distribution function: from the area under a Brownian excursion to the maximal height of fluctuating interfaces *J. Stat. Phys.* **119** 777
[162] Majumdar S N and Krapivsky P L 2003 Extreme value statistics and traveling fronts: various applications *Physica* A **318** 161
[163] McCabe J and Ouvry S 1991 Perturbative three-body spectrum and the third virial coefficient in the anyon model *Phys. Lett.* B **260** 113
[164] McKane A J and Tarlie M B 1995 Regularization of functional determinants using boundary perturbations *J. Phys. A: Math. Gen.* **28** 6931
[165] McKean H P 1994 A limit law for the ground state of Hill's equation *J. Stat. Phys.* **74** 1227
[166] Mello P A, Pereyra P and Kumar N 1988 Macroscopic approach to multichannel disordered conductors *Ann. Phys., NY* **181** 290
[167] Molčanov S A 1981 The local structure of the spectrum of the one-dimensional Schrödinger operator *Commun. Math. Phys.* **78** 429
[168] Montambaux G and Akkermans E 2005 Non exponential quasiparticle decay and phase relaxation in low dimensional conductors *Phys. Rev. Lett.* **95** 016403
[169] Monthus C 1995 Étude de quelques fonctionnelles du mouvement brownien et de certaines propriétés de la diffusion unidimensionnelle en milieu aléatoire *PhD Thesis* Université Paris 6 *Ann. Phys. (France)* **20** 341
[170] Monthus C and Comtet A 1994 On the flux distribution in a one-dimensional disordered system *J. Phys.* I *(France)* **4** 635–53
[171] Monthus C, Oshanin G, Comtet A and Burlatsky S 1996 Sample-size dependence of the ground-state energy in a one-dimensional localization problem *Phys. Rev.* E **54** 231
[172] Nersesyan A A, Tsvelik A M and Wenger F 1994 Disorder effects in two-dimensional d-wave superconductors *Phys. Rev. Lett.* **72** 2628
[173] Oshanin G, Mogutov A and Moreau M 1993 Steady flux in a continuous-space Sinai chain *J. Stat. Phys.* **73** 379
[174] Ossipov A and Fyodorov Y V 2005 Statistics of delay times in mesoscopic systems as a manifestation of eigenfunction fluctuations *Phys. Rev.* B **71** 125133
[175] Ouvry S 1994 δ perturbative interactions in Aharonov–Bohm and anyons models *Phys. Rev.* D **50** 5296
[176] Ovchinnikov A A and Erikmann N S 1977 Density of states in a one-dimensional random potential *Sov. Phys.—JETP* **46** 340
[177] Pascaud M 1998 Magnétisme orbital de conducteurs mésoscopiques désordonnés et propriétés spectrales de fermions en interaction *PhD Thesis* Université Paris 11
[178] Pascaud M and Montambaux G 1999 Persistent currents on networks *Phys. Rev. Lett.* **82** 4512
[179] Perman M and Wellner J A 1996 On the distribution of Brownian areas *Ann. Appl. Probab.* **6** 1091
[180] Pierre F, Gougam A B, Anthore A, Pothier H, Esteve D and Birge N O 2003 Dephasing of electrons in mesoscopic metal wires *Phys. Rev.* B **68** 085413
[181] Pitman J and Yor M 1986 Asymptotic laws of planar Brownian motion *Ann. Probab.* **14** 733
[182] Rammer J and Shelankov A L 1987 Weak localization in inhomogeneous magnetic fields *Phys. Rev.* B **36** 3135
[183] Rice S O 1982 The integral of the absolute value of the pinned Wiener process—calculation of its probability density by numerical integration *Ann. Probab.* **10** 240
[184] Richard C 2003 Area distribution of the planar random loop boundary *J. Phys. A: Math. Gen.* **37** 4493
[185] Roth J-P 1983 Le spectre du Laplacien sur un graphe *Colloque de Théorie du Potentiel—Jacques Deny* (Paris: Orsay) p 521
[186] Roth J-P 1983 Spectre du Laplacien sur un graphe *C. R. Acad. Sci. Paris* **296** 793
[187] Rudenberg K and Scherr C 1953 *J. Chem. Phys.* **21** 1565
[188] Schmidt H 1957 Disordered one-dimensional crystals *Phys. Rev.* **105** 425
[189] Schomerus H and Titov M 2003 Band-center anomaly of the conductance distribution in one-dimensional Anderson localization *Phys. Rev.* B **67** 100201
[190] Selberg A 1956 Harmonic analysis and discontinuous groups in weakly symmetric Riemannian spaces, with applications to Dirichlet series *J. Ind. Math. Soc.* **20** 47
[191] Shapiro B 1982 Renormalization-group transformation for the Anderson transition *Phys. Rev. Lett.* **48** 823
[192] Shapiro B 1983 Quantum conduction on a Cayley tree *Phys. Rev. Lett.* **50** 747
[193] Sharvin D Yu and Sharvin Yu V 1982 Magnetic-flux quantization in a cylindrical film of a normal metal *JETP Lett.* **34** 272
[194] Shelton D G and Tsvelik A M 1998 Effective theory for midgap states in doped spin-ladder and spin Peierls systems: Liouville quantum mechanics *Phys. Rev.* B **57** 14242
[195] Shepp L A 1982 On the integral of the absolute value of the pinned Wiener process *Ann. Probab.* **10** 234
Shepp L A 1991 Acknowledgement of priority *Ann. Probab.* **19** 1397

[196] Smith F T 1960 Lifetime matrix in collision theory *Phys. Rev.* **118** 349
[197] Stark H M and Terras A A 1996 Zeta functions of finite graphs and coverings *Adv. Math.* **121** 124
[198] Steiner M, Chen Y, Fabrizio M and Gogolin A O 1999 Statistical properties of localization–delocalization transition in one dimension *Phys. Rev.* B **59** 14848
[199] Steiner M, Fabrizio M and Gogolin A O 1998 Random mass Dirac fermions in doped spin-Peierls and spin-ladder systems: one-particle properties and boundary effects *Phys. Rev.* B **57** 8290
[200] Takayama H, Lin-Liu Y R and Maki K 1980 Continuum model for solitons in polyacetylene *Phys. Rev.* B **21** 2388
[201] Tanner G 2001 Unitary-stochastic matrix ensembles and spectral statistics *J. Phys. A: Math. Gen.* **34** 8485
[202] Tanner G 2005 From quantum graphs to quantum random walks, unpublished (*Preprint* quant-ph/0504224)
[203] Texier C 1999 Quelques aspects du transport quantique dans les systèmes désordonnés de basse dimension *PhD Thesis* Université Paris 6, available at http://ipnweb.in2p3.fr/∼lptms/membres/texier/research.html
[204] Texier C 2000 Individual energy level distributions for one-dimensional diagonal and off-diagonal disorder *J. Phys. A: Math. Gen.* **33** 6095–128
[205] Texier C 2002 Scattering theory on graphs (2): the Friedel sum rule *J. Phys. A: Math. Gen.* **35** 3389–407
[206] Texier C and Büttiker M 2003 Local Friedel sum rule in graphs *Phys. Rev.* B **67** 245410
[207] Texier C and Comtet A 1999 Universality of the Wigner time delay distribution for one-dimensional random potentials *Phys. Rev. Lett.* **82** 4220–3
[208] Texier C and Degiovanni P 2003 Charge and current distribution in graphs *J. Phys. A: Math. Gen.* **36** 12425–52
[209] Texier C and Montambaux G 2001 Scattering theory on graphs *J. Phys. A: Math. Gen.* **34** 10307–26
[210] Texier C and Montambaux G 2004 Weak localization in multiterminal networks of diffusive wires *Phys. Rev. Lett.* **92** 186801
[211] Texier C and Montambaux G 2005 Dephasing due to electron–electron interaction in a diffusive ring, unpublished (*Preprint* cond-mat/0505199) (*Phys. Rev.* B, at press)
[212] Texier C and Montambaux G 2005 Quantum oscillations in mesoscopic rings and anomalous diffusion *J. Phys. A: Math. Gen.* **38** 3455–71
[213] Thornton T J, Pepper M, Ahmed H, Andrews D and Davies G J 1986 One-dimensional conduction in the 2D electron gas of a GaAs–AlGaAs heterojunction *Phys. Rev. Lett.* **56** 1198
[214] Tracy C A and Widom H 1993 Level-spacing distribution and the Airy kernel *Phys. Lett.* B **305** 115
[215] Tracy C A and Widom H 2002 Distribution functions for largest eigenvalues and their applications *Proc. ICM (Beijing)* vol 1, p 587
[216] Verbaarschot J 1994 The spectrum of the Dirac operator near zero virtuality for $N_c = 2$ and chiral random matrix theory *Nucl. Phys.* B [FS] **426** 559
[217] Verwaat W 1979 On a stochastic difference equation and a representation of non negative infinitely divisible random variables *Adv. Appl. Probab.* **111** 750
[218] Vidal J, Montambaux G and Douçot B 2000 Transmission through quantum networks *Phys. Rev.* B **62** R16294
[219] Wegner F 1979 The mobility edge problem: continuous symmetry and a conjecture *Z. Phys.* B **35** 207
[220] Wegner F 1983 Exact density of states for lowest Landau level in white noise potential: superfield representation for interacting systems *Z. Phys. B: Condens. Matter* **51** 279
[221] Wegner F J 1976 Electrons in disordered systems: scaling near the mobility edge *Z. Phys.* B **25** 327
[222] Weiss G H and Havlin S 1986 Some properties of a random walk on a comb structure *Physica* A **134** 474
[223] Werner W 1994 Sur les points autour desquels le mouvement Brownien plan tourne beaucoup *Probab. Theory Rel.* **99** 111
[224] Wind S, Rooks M J, Chandrasekhar V and Prober D E 1986 One-dimensional electron–electron scattering with small energy transfers *Phys. Rev. Lett.* **57** 633
[225] Winn B 2003 The Laplacian on a graph and quantum chaology *PhD Thesis* University of Bristol, available at http://www.math.tamu.edu/∼bwinn/thesis.htm
[226] Wu F Y and Kunz H 1999 Restricted random walks on a graph *Ann. Combin.* **3** 475
[227] Yor M 1980 Loi de líndice du lacet Brownien et distribution de Hartman–Watson *Z. Wahrscheinlichkeit.* **53** 71
[228] Yor M 2000 *Exponential Functionals of Brownian Motion and Related Processes* (Berlin: Springer)
[229] Zirnbauer M R 1996 Riemannian symmetric superspaces and their origin in random-matrix theory *J. Math. Phys.* **37** 4986